Planta (1995) 197: 655–671

Planta

Protons and calcium modulate SV-type channels in the vacuolar-lysosomal compartment – channel interaction with calmodulin inhibitors

Barbara Schulz-Lessdorf, Rainer Hedrich

Institut für Biophysik, Universität Hannover, Herrenhäuser Strasse 2, D-30419 Hannover, Germany

Received: 20 February 1995/Accepted: 26 May 1995

Abstract. *S*lowly *a*ctivating *v*acuolar (SV-type; Hedrich and Neher 1987, *Nature* 329: 833–835) ion channels provide the predominant membrane conductance of the vacuolar-lysosomal compartment of *Vicia faba* L. guard cells and sugar beet (*Beta vulgaris* L.) taproots. Applying the patch-clamp technique to isolated vacuoles of both tissues, the electrical and pharmacological properties of guard-cell SV-type currents were studied and compared to the sugar beet channel with regard to its modulation by cytoplasmic Ca^{2+} and pH. This outward rectifier of *V. faba* guard cells showed a half-maximum activation at 55–60 mV with an apparent gating charge equivalent of $z \approx 4$. Studies on the single-channel and whole-vacuole level revealed an extremely high conductance of 280 pS for the guard-cell channels at a mean density of 0.37 μm^{-2} compared to taproots (120–140 pS at about 0.16 channels per μm^2). Guard-cell SV-type channels are weakly selective for cations over anions and lack saturation at KCl concentrations of up to 1 M. Since in the absence of physiological K^+ concentrations, Ca^{2+} is the major permeable ion, relative changes in the amounts of the two ions might control the permeation process. In spite of their different origins and physiological functions, in guard cells and beet taproot cells, cytoplasmic Ca^{2+} and protons, both considered as candidates for intracellular signalling in plants, modulate the voltage dependence of SV-type channels. While the two effectors do not alter the single-channel conductance, they strongly interact with the voltage sensor. The calmodulin (CaM) antagonists N-(6-aminohexyl)-5-chloro-1-naphthalenesulfonamide hydrochloride (W-7), trifluoperazine (TFP) and calmidazolium hydrochloride (R 24571) effectively blocked the channel in an antagonist-specific manner. In agreement with the properties of a Ca^{2+}-permeable channel, CaM could be involved in the modulation of the activation threshold of the SV-type channel. We therefore conclude that guard-cell SV-type channels, which might be responsible for the release of K^+, Cl^- and to a smaller extent Ca^{2+} during stomatal closure, could serve as an intracellular sensor for changes in cytosolic calcium (calcium-CaM) and pH.

Key words: Calcium – Calmodulin antagonists – pH – SV-type channels (vacuole) – Taproot, guard cells

Introduction

The major tasks of the vacuolar-lysosomal compartment are storage and mobilisation of ions (e.g. Ca^{2+}, K^+, Cl^-) and metabolites (e.g. malate and sugars), processes which are involved in regulation of cell volume and turgor (Matile 1978). Vacuolar ion and metabolite transport are mediated by ion channels, carriers and electrogenic proton pumps (Hedrich et al. 1986*a*; Hedrich and Schroeder, 1989). Initial patch-clamp studies on sugar beet vacuoles identified outward[1]-rectifying SV-type channels (slowly activating vacuolar channels) and weakly voltage-dependent FV-type (= fast activating vacuolar) channels of low selectivity for cations over anions (P_K: $P_{Cl} \approx 6$) which have been considered as pathways for vacuolar anion and cation transport (Hedrich and Neher 1987). The SV-type channels are widely distributed in plants. They have been discovered in the vacuolar-lysosomal membrane of all cell types studied, such as those in the leaf, root, liverwort thallus, aleurone layer and cultured cells, and are therefore

Abbreviations: CaM = calmodulin; $Gluc^-$ = gluconate; DIDS = 4,4,-diisothiocyano-2,2-stilbenedisulfonic acid; Mes = 2-(N-morpholino)-ethanesulfonic acid; R 24571 = calmidazolium hydrochloride; SV = slowly activating vacuolar; TEA^+ = tetraethylammonium; TFP = trifluoperazine; W-7 = N-(6-aminohexyl)-5-chloro-1-naphthalenesulfonamide hydrochloride

Correspondence to: R. Hedrich; FAX: 49 (511) 7622606; Tel.: 49 (511) 7622603

[1] According to the sign convention for endomembranes, the vacuolar lumen is considered electrically equivalent to the extracellular space (Bertl et al. 1992; cf. method section!)

suggested to be ubiquitous in higher plants[2] (Hedrich et al. 1988). Voltage-dependent and voltage-independent vacuolar currents of slow and fast kinetics were further distinguished by their Ca^{2+} sensitivity (Hedrich and Neher 1987; Schroeder and Hedrich 1989). Increasing the cytosolic Ca^{2+} concentration to > 0.3 μM resulted in an increase in the relative contribution of SV-type channels to the macroscopic current. Elevated cytoplasmic Ca^{2+} levels are supposed to result from Ca^{2+} influx through the plasma membrane (Schroeder and Hagiwara 1989; Cosgrove and Hedrich 1991; Thuleau et al. 1994) or vacuolar channels. Gadolinium (Gd^{3+})-sensitive Ca^{2+} channels (Johannes et al. 1992; Allen and Sanders 1994a) and inositoltrisphosphate-activated Ca^{2+} channels (Alexandre et al. 1990; Allen and Sanders 1994b) might catalyze Ca^{2+} release from the vacuole. At rest, due to the abundance and activity of H^+-pumping V-type ATPases and the vacuolar PP_iases, vacuolar membrane potentials around -10 to -40 mV are assumed (Sze 1985; Coyaud et al. 1987; Hedrich et al. 1989). However, SV-type channels activate at positive membrane potentials. Since the equilibrium potential for Ca^{2+} across the vacuolar membrane is more positive than 200 mV, a vacuolar Ca^{2+} release into the cytosol could depolarize the membrane potential to the threshold of SV-channel activation (Sanders et al. 1990). Recently a voltage-independent, Ca^{2+}-activated K^+ channel in the vacuolar membrane of guard cells with features similar to the FV-type channel in sugar beet vacuoles (Hedrich and Neher 1987) was suggested to be linked to the activation of the SV-type channel (Ward and Schroeder 1994). In the light of the high K^+ concentration in the vacuolar lumen and the cytosol, however, the role of this channel in pre-depolarization remains unclear.

Volume and turgor changes during reversible cell expansion or growth require coordination of metabolite and ion fluxes between the vacuolar and the plasma membrane (Schulz-Lessdorf et al. 1994). These processes, which are often triggered by plant hormones, involve cytoplasmic Ca^{2+} and protons for signal transduction (Gehring et al. 1990; Blatt 1992; Irving et al. 1992; Blatt and Armstrong 1993, Lemtiri-Chlieh and MacRobbie 1994; Ward and Schroeder 1994). Because of the lack of detailed information about the regulation of vacuolar transport on the one side, and common second messengers coupling plasma membrane and vacuolar ion fluxes in response to cell volume regulators on the other, we focussed on the modulation of SV-type channels in guard-cell and sugar beet vacuoles by Ca^{2+}, calmodulin (CaM) antagonists and protons. Both cell types are characterized by different ion transport properties reflecting their unique physiological tasks: (i) seasonal changes in vacuolar anion and cation contents during sugar storage and mobilization of beet taproots (Perry et al. 1987); (ii) rapid changes in amplitude and direction of ion fluxes which drive stomatal movement in guard cells within minutes in response to different stimuli, e.g. light, phytohormones and CO_2 (Raschke 1979; Irving et al. 1992). The elucidation of channel density and cell/tissue-specific features of the SV-type channel from both plant origins may help to better understand its physiological role. Therefore, in the following, the intrinsic properties of the guard-cell channel were analysed with respect to voltage dependence, selectivity and pharmacology before the modulation of the SV-type channel by Ca^{2+}, pH and CaM antagonists was compared in guard-cell and sugar beet vacuoles.

[2] It should be noted that yeast vacuoles contain a slowly activating cation channel with a voltage dependence inverse to the SV-type channel (Bertl and Slayman 1990)

Materials and methods

Isolation of guard-cell vacuoles. Guard cell vacuoles were isolated from enzymatically prepared protoplasts of broad beans (*Vicia faba* L. cv Weißkernige Hangdown, Gebag, Hannover, Germany) grown in the greenhouse or botanical garden of the Universities of Göttingen and Hannover. Epidermal peels with intact guard cells were isolated from four to six leaflets of 10–14-d-old plants by disintegration for 3×15 s in a Waring blendor with cold washes through a 200-μm nylon net in between. Stomata were exposed overnight to lytic enzymes at 18°C for cell wall degradation and release of guard-cell protoplasts. The enzyme solution was composed of 2% Cellulase R-10 (Yakult, Tokyo, Japan), 1% Macerocyme R-10 (Yakult, Tokyo, Japan) 0.5% bovine serum albumin (BSA), 1 mM $CaCl_2$ and 10 mM Na-ascorbate (adjusted to pH 5.5 with HCl) adjusted to 400 mosmol·kg^{-1} with D-sorbitol (Raschke and Hedrich 1989). Protoplasts added to a 200-μl recording chamber sedimented and adhered to its glass bottom while exposed to an isotonic bathing solution. Guard-cell vacuoles were released from protoplasts by controlled osmotic shock with a hypotonic solution introduced by application pipettes with tip diameters of 4–6 μm (Fig. 1; cf. the section *Solutions* below). To reduce capillary forces, the pipettes were inside coated with Sigmacote (Sigma, Deisenhofen, Germany). Application pipettes were positioned close to the chosen protoplasts. While the recording chamber was perfused with bathing solution at a rate of 1.9 ml·min^{-1}, continuous pipette efflux of hypotonic solution caused protoplast swelling and, after 3–5 min, disintegration of the plasma membrane. Freshly extruded vacuoles adhered to the chamber bottom, were osmotically stabilized, and immediately (≤ 2 min) used for the experiment. This fast method of isolating guard-cell vacuoles from single preselected protoplasts was used to reduce loss of cytosolic or loosely membrane-bound cofactors.

Isolation of sugar beet vacuoles. Sugar beet (*Beta vulgaris* L.) vacuoles were mechanically isolated according to the method of Coyaud et al. (1987) from five to nine month-old sugar beet taproots grown in the greenhouse or fields surrounding Göttingen. Thin slices were cut off from storage tissue with a razor blade. Slice surfaces were rinsed with bathing solution. Vacuoles extruding from cut cells were collected into the recording chamber. Cell debris was removed by bath perfusion.

Solutions. The hypotonic solution used for vacuole release from guard-cell protoplasts was composed of 100 mM KCl, 2 mM EGTA, 5 mM $MgCl_2$, and 5 mM Tris/2-(N-morpholino)ethanesulfonic acid (Mes) pH 7.5 ($\pi \approx 200$ mosmol·kg^{-1}). All patch-clamp experiments were performed at temperatures of 293–303 K. Unless otherwise specified in the figure legends or the text, the solutions used contained 2–200 mM KCl, 1 mM $CaCl_2$, 0.5–5 mM $MgCl_2$, 5 mM Tris/Mes pH 7.5 in the bath and pipette. The Ca^{2+} permeability of the SV-type channel was determined with 0.1 and 1 mM $CaCl_2$ ($\pm$ 100 mM KCl) in the bath and with 10 mM $CaCl_2$ ($\pm$ 100 mM KCl) in the pipette; each solution was buffered with 5 mM Tris/Mes to pH 7.5. D-Sorbitol was added to adjust the final osmolality to $\pi \approx 400$ mosmol·kg^{-1} for analysis of the guard-cell SV-type channel, and to values 100–150 mosmol·kg^{-1} more than the osmotic pressure of taproots for the sugar beet channel. Osmolalities were verified by a vapour-pressure osmometer (5500; Wescor, Logan, Utah, USA). N-(6-Aminohexyl)-5-chloro-1-naphtalenesulfonamide

hydrochloride (W-7) and trifluoperazine (TFP) were dissolved in water, and stock solutions of 4,4-diisothiocyano-2,2-stilbenedisulfonic acid (DIDS) and calmidazolium hydrochloride (R 24571) in dimethylsulfoxide (DMSO). Dimethylsulfoxide did not affect SV-type channels up to 0.2% final concentration.

Wheat-germ CaM was isolated by acetone extraction, heat denaturation and subsequent chromatography on diethylaminoethyl (DEAE)-cellulose and fluphenazine-Sepharose columns according to the method of Anderson (1983). The affinity-column eluate was desalted on a DEAE-column. Subsequently, CaM was eluted using Tris-buffer (1 mM EGTA in 10 mM Tris/Mes pH 7.5) and dialyzed against 10 mM Tris/Mes pH 7.5 before use. Calmodulin concentration was determined by modified Bradford assay (Biorad, München, Germany) and the activity monitored by phosphodiesterase activation (Wallace et al. 1983). Bovine-brain and spinach CaM were purchased from Sigma.

Patch-clamp recordings and data aquisition. Patch pipettes were sealed against the vacuolar membrane to study ionic currents in the whole-vacuole configuration (analogous to the whole-cell configuration; Hamill et al. 1981) and in excised membrane patches. Kimax-51 glass capillaries (Kimble products, Vineland, N.Y., USA) were coated on the inside with Sigmacote (Sigma) and pulled in two steps to produce patch pipettes with tip-diameters of 1–3 μm (corresponding to 3–8 MΩ in 200 mM KCl). Sigmacote treatment of the patch-pipette interior prevented the creeping of sealed membranes into the pipette, a process often followed by membrane rupture. The external glass surfaces of the pipette tips were coated with Sylgard 184 (Dow corning, Midland, Mich., USA) and the rims were fire-polished. Current recordings were performed in the voltage-clamp mode using an EPC-7 or EPC-9 patch-clamp amplifier (List electronic, Darmstadt, and HEKA, Lambrecht, Germany). Whole-vacuole and single-channel currents were low-pass-filtered with an eight-pole Bessel filter at 100–500 Hz and 2–5 kHz, respectively, digitized at a sample rate of 0.1–1 ms (VR 10 CRC Instrutech Corp., New York, N.Y., USA), and stored on hard disk or videotape. The membrane potentials were corrected for liquid-junction potentials and series resistances (1.1 MΩ $\leq R_S \leq$ 3.3 M; $|I| \leq$ 13 nA; 4 pF $\leq c \leq$ 28 pF; Neher 1992). In solutions mainly composed of KCl, liquid-junction potentials were nominally absent.

Sign convention. According to the sign convention for electrical measurements on single biomembrane-covered endosomes (Bertl et al. 1992) the vacuolar membrane potential denotes the potential difference between the cytoplasmic and the lumen (out)side of the membrane:

$$U = U_{cytosol} - U_{lumen}; \quad U_{lumen} = 0.$$

Consequently, membrane patches exposing the cytoplasmic surface to the bath solution reflect the inside-out configuration.

Data analysis. Single-channel events were analysed on an Atari Mega ST4 with the program TAC of Instrutech Corp. using the 50%-threshold method for determination of single-channel open and closed times (Colquhoun and Sigworth 1983; Sigworth 1983). All channel events within 1 min, or at least 400 events per current trace, were analysed for determination of the channel activities, amplitudes and mean open times. Channel activity has been defined as the open probability (P_o) of all (= N) channels in an excised membrane patch. This product $N \cdot P_o$ was determined as the sum of individual open dwell times (t_{oi}) in level i, multiplied by the number of single-channel amplitudes superimposed, divided by the total time (t_{total}), according to Sigworth (1983, Eq. 1):

$$N \cdot P_o = \frac{\sum_{i=1}^{N} t_{oi} \cdot n(t_{oi})}{t_{total}} \qquad \text{(Eq. 1)},$$

Analysis of whole-vacuole currents was performed using the program REVIEW (Instrutech Corp). Activation curves for SV-type currents were fitted by a single Boltzmann distribution (Eq. 2) using the program SIGMAPLOT (Jandel Scientific, Erkrath, Germany).

$$\frac{I_{ss}}{I_{tail}} = \frac{g}{g_{max}} = \frac{N \cdot P_o}{(N \cdot P_o)_{max}} = \frac{1}{(1 + \exp[(U_{0.5} - U) \cdot ze/kT])} \qquad \text{(Eq. 2)}$$

where U = membrane potential; e = elementary charge; k = Boltzmann constant; T = absolute temperature. The midpoint potential of current activation ($U_{0.5}$) and gating charge (z) were determined from the channel activities normalized to the maximal activity ($N \cdot P_o/(N \cdot P_o)_{max}$), and from the conductance ratio (g/g_{max}) which reflects the open probability extracted from the ratio of whole-vacuole steady-state currents (I_{ss}) versus corresponding tail-current amplitudes (I_{tail}) at t = 0. For the analysis of channel selectivity the reversal potentials were determined by interpolation of the single-channel current amplitudes and of the slope of whole-vacuole tail currents. Nernst potentials for K^+, Ca^{2+} and Cl^- were calculated using ionic activities derived from the ion concentrations according to Robinson and Stokes (1959).

Results

Voltage dependence of the guard-cell SV-type channel. Patch-clamp experiments were performed on vacuoles released by selective osmotic shock (Fig. 1) from *Vicia faba* guard-cell protoplasts. Holding the membrane potential at 0 mV, 4-s voltage pulses from 76 to − 30 mV elicited time-dependent, outward-rectifying whole-vacuole currents of the SV-type (Fig. 2A), well known from vacuoles of other tissues (Hedrich et al. 1986b, 1988; Colombo et al. 1988; Maathuis and Prins 1991a, b). Single-channel analysis on inside-out patches excised from the whole-vacuole configuration and exposed to 200/20 mM KCl (bath/pipette), 1 mM $CaCl_2$, 5 mM $MgCl_2$, 5 mM Tris/Mes pH 7.5, identified a voltage-dependent 281 ± 20 pS (mean ± SSD) channel as the major vacuolar conductance (Fig. 2B; $n = 15$). In addition, channels of 38 ± 3 pS, 82 ± 3 pS and 131 ± 17 pS were observed ($n = 4$, $n = 3$ and $n = 6$, respectively; data not shown). Clamping the membrane potential to values positive to 10 mV resulted in a voltage-dependent activation of single 280 pS-channels (Fig. 2B), whereas almost no single-channel fluctuations were detected at negative membrane potentials (Fig. 2C, open circles). In order to analyse whether or not the single 280 pS-channels constituted the macroscopic SV-type current, in Fig. 2C we superimposed (i) the single channel amplitude- and channel activity-voltage curves, (ii) the current-voltage curve of the membrane patch derived from these single-channel characteristics (cf. Eq. 3), and (iii) the whole-vacuole currents (cf. Fig. 2A and Eq. 3).

$$I(U) = i(U) \cdot N \cdot P_o(U) \qquad \text{(Eq. 3)};$$

where I is the normalized current of the whole membrane patch or whole vacuole, respectively; i is the current through a single open channel at clamp voltage U (Fig. 2C, open triangles), P_o the voltage-dependent open probability, and N the channel number in the patch or the whole vacuolar membrane, respectively (Aldrich and Yellen 1983). The striking coincidence in the voltage dependence of normalized currents derived from single-channel events (Fig. 2c, filled squares) and whole-vacuole recordings measured (Fig. 2c, filled circles), identified the

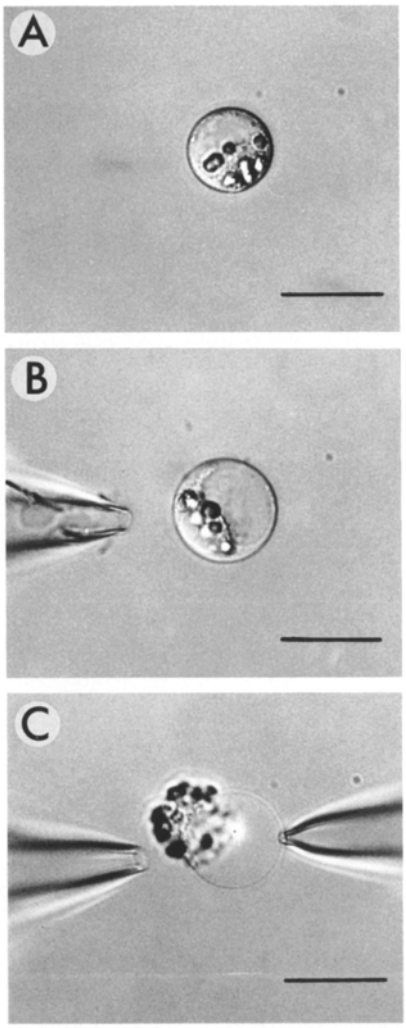

Fig. 1A–C. Isolation of guard-cell vacuoles. **A** Protoplast of *Vicia faba*. **B** Osmotic swelling of the protoplast by application of hypotonic solution (pipette on the left). **C** Due to the osmotic shock the plasma membrane of the protoplast collapsed and the vacuolar membrane became accessible for patch-clamp studies (patch pipette right-hand side). Bar = 20 μm

large-conductance channel as the SV-type homologue of guard cells. Therefore, under the experimental conditions given here, the smaller conductances seem not to contribute significantly to the whole-vacuole currents (Fig. 2C) and were not analysed further. When the activity-voltage curves obtained from single-channel fluctuations and whole-vacuole currents were described using a first-order Boltzmann equation (Eq. 2), we calculated a midpoint potential of activation of 57.3 ± 4.6 mV ($n = 7$, mean ± SSD) and an elementary charge equivalent of 3.9 ± 0.6 ($n = 11$) under standard conditions (ionic concentrations given in mM in bath and pipette solutions: 20–200 KCl, 1 $CaCl_2$, 5 $MgCl_2$, 5 Tris/Mes pH 7.5).

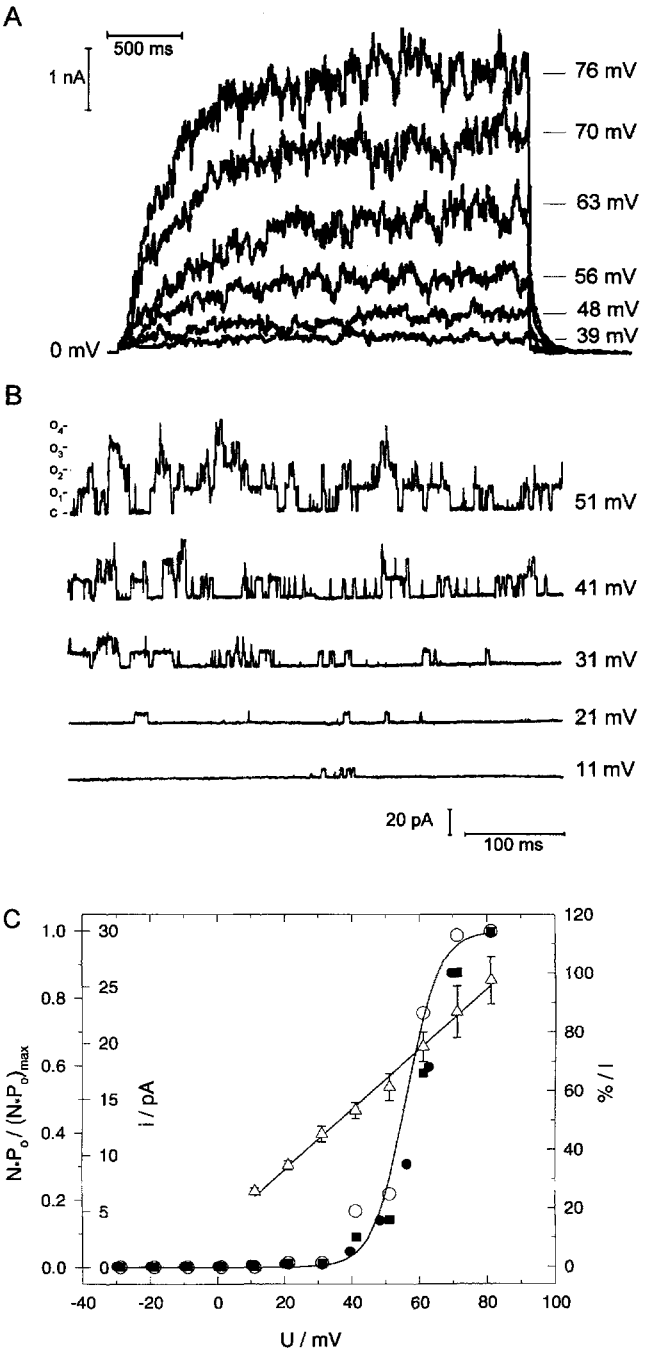

Fig. 2A–C. Voltage dependence of SV-type currents in the vacuolar membrane of *V. faba* guard cells. **A** Whole-vacuole currents were induced by application of single voltage pulses from 76 to − 30 mV (cytoplasmic side relative to lumen side). Six individual current traces were superimposed. **B** Voltage-dependent activation of single 280 pS-channels in an inside-out membrane patch. *c*, channels closed; o_n, n channels open. **C** Identification of the 280 pS-conductance as the SV-type channel in guard-cell vacuoles. Voltage-dependent channel activities [= the open probability of all channels in the patch, (○), $N \cdot P_o$] and channel amplitudes (i, △) were determined from the single-channel recordings shown in B. Macroscopic currents reconstructed (■) from the single-channel events according to the equation $I(U) = i(U) \cdot N \cdot P_o(U)$ and whole-vacuole currents measured in A (●) are shown as a function of the membrane potential and normalized to their amplitudes at 70 mV. The strong similarity if not identity of the voltage dependence of calculated and recorded steady-state currents rendered the identification of the 280 pS-conductance as the SV-type channel of guard cells. Voltage dependence of the open probability was fitted by a single exponential Boltzmann equation with a midpoint potential of 56 mV and a gating charge of 4.9. Major electrolytes in the bath/pipette solutions were 200/20 mM KCl

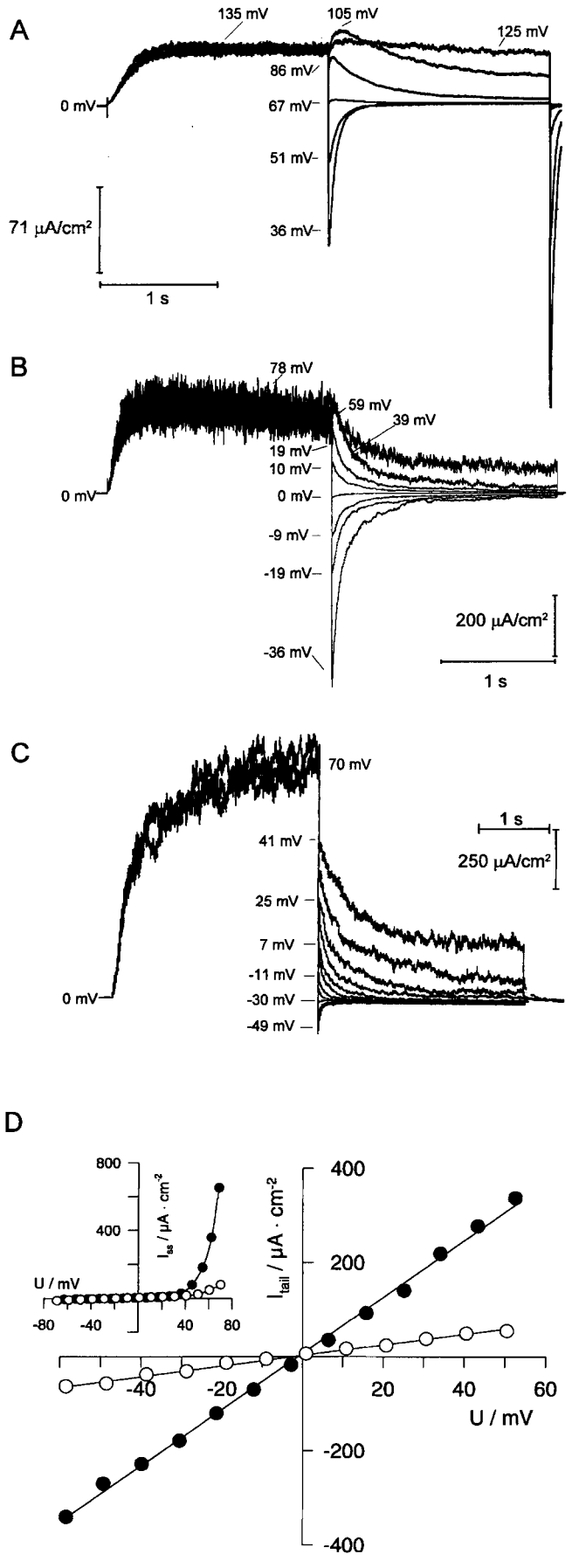

Selectivity. From previous studies, in which physiological K^+ concentrations were replaced by unphysiological Ca^{2+} concentrations, SV-type channels have been assumed to represent vacuolar Ca^{2+}-induced Ca^{2+}-release channels or even Ca^{2+}-uptake channels (Pantoja et al. 1992; Ward and Schroeder 1994). In order to elucidate the charge carriers of the guard-cell SV-type current, the relative ion permeability of the channel was determined in various media containing Ca^{2+}, K^+ and Cl^-. For this, double-voltage pulse sequences were applied to whole guard-cell vacuoles and the resulting tail currents were analysed to determine the reversal potential (Fig. 3).

In a first approach, 10 mM $CaCl_2$ was presented in the pipette and 0.1 or 1 mM $CaCl_2$ in the bath. By choice of these transmembrane Ca^{2+} gradients the physiological Ca^{2+} concentrations in the immediate neighborhood (≤ 0.2 µm, cf. Roberts et al. 1990) of an open vacuolar Ca^{2+} channel (cf. Allen and Sanders 1994a), which are assumed to rise up to 1 mM during Ca^{2+} transients (Hille 1992), were imitated. Indeed, under these conditions in the absence of K^+ on both membrane sides, SV-type currents reversed at 61.1 ± 3.2 mV ($n = 6$; Fig. 3A) and 32.5 ± 0.7 mV ($n = 3$) in agreement with the calculated Nernst potential for Ca^{2+} (58.9 and 30.4 mV, respectively). This indicated that in the presence of Ca^{2+} and Cl^- the SV-type channel is Ca^{2+}-selective.

When, however, the ionic conditions in vivo were simulated adding a symmetrical background of 100 mM KCl plus 0.5 mM $MgCl_2$, SV-type currents reversed at -0.7 ± 0.6 mV (Fig. 3B; $n = 3$), indicating that permeation of ions other than just Ca^{2+} determined the reversal potential. This result is in striking contrast to the relative permeability ratio $P_{Ca}:P_K$ of 5.3 determined for the guard-cell SV-type channel by Ward and Schroeder (1994). According to that value and constant field assumptions one would predict a zero-current potential of 14 mV instead of -0.7 mV for the ionic conditions used in Fig. 3B. Similar large discrepancies between reversal potentials measured and expected were determined under

Fig. 3A–D. Selectivity of the *V. faba* guard-cell SV-type channel determined by tail-current analysis. Double-voltage pulse sequences were applied to whole vacuoles from a holding potential of 0 mV. The SV-type currents were activated by a prepulse to depolarized potentials and declined in response to instantaneous voltage steps to the potentials indicated. **A** With 0.1 mM and 10 mM $CaCl_2$ in bath and pipette solution, respectively, the SV-type channel reversed at 61.1 ± 3.2 mV ($n = 6$, mean $\pm$ SD) as expected from a Ca^{2+}-selective channel. **B** Under the same conditions as in **A**, but against a background of 100 mM KCl on both membrane sides, tail currents reversed at 1 mV (see text). **C** In the presence of 200/20 mM KCl (bath/pipette) and symmetrical 1 mM Ca^{2+} the reversal potential $U_{rev} = -26$ mV of SV-type currents revealed a relative permeability ratio $P_K:P_{Cl}:P_{Ca} \approx 1:0.3:0.1$. Tail currents were evoked after preactivation of the outward rectifier at 70 mV by voltage steps to (from top to bottom) 41 mV, 33 mV, 25 mV, 15 mV, 7 mV, -3 mV, -11 mV, -20 mV, -30 mV, -39 mV and -49 mV. **D** Tail-current/voltage curves in the presence of 100/100 mM KCl (●) in bath and pipette and after replacement by 100 K-gluconate (○) in the bath. The reversal potential of tail currents shifted from 0 mV to -5 ± 1 mV ($n = 3$) and thus revealed a $P_K:P_{Cl}:P_{Gluc} \approx 1:0.3:(<0.1)$ (see Table 1, text and *Appendix*). In the presence of $Gluc^-$ the steady-state currents (*Inset*) as well as tail currents were reduced by 80–90%.

Table 1. Comparison of SV-current reversal potentials (U_{rev}) measured under multiionic conditions and values predicted (U''_{rev}) in the assumption of a channel permeability for Ca^{2+} and K^+ only. Chloride was applied as counterion for all cations (see *Materials and methods*). A relative permeability ratio $P_K/P_{Ca} = 0.2$, as proposed by Ward and Schroeder (1994), was assumed for prediction of the reversal potential (U''_{rev}), which was calculated by use of Eq. 23 with $P_{Cl} = 0$

	$[K^+]_o$* (mM)	$[K^+]_i$* (mM)	$[Ca^{2+}]_o$* (mM)	$[Ca^{2+}]_i$* (mM)	U_{rev}(mV) ($\pm$ SD)	U''_{rev} (mV) ($P_K:P_{Ca} = 0.2$)
1	200	2	1	1	30 ± 3 ($n = 4$)	59
2	200	0	1	1	30 ($n = 1$)	62
3	20	200	1	1	-25.5 ± 0.9 ($n = 3$)	-44
4	100	100	10	0.1	-0.7 ± 0.6 ($n = 3$)	14
5	150	150	5	0.1	0 ($n = 2$)	6

* Note that ion concentrations rather than activities were used for calculations of U''_{rev} (cf. Table 3)

five different transmembrane K^+/Ca^{2+} ratios (Table 1). These results showed that SV-type currents were not carried exclusively by Ca^{2+} and K^+ but, in line with our previous findings, anions have to be taken into account, too (Hedrich and Schroeder 1989 for review).

In the following, each ion species of the bath and pipette solution was examined with respect to its ability to permeate the channel pore. Table 2 indicates the relative ion permeabilities of SV-type channels with respect to K^+, Ca^{2+}, tetraethylammonium (TEA^+), Cl^-, and gluconate$^-$ (Gluc) which were analysed from reversal-potential measurements under seven different transmembrane ionic gradients. Thereby, the permeability coefficients P_K, P_{Cl}, P_{Ca}, P_{TEA} and P_{Gluc} were fitted according to the constant-field theory (cf. *Appendix*). The reversal potentials, U_{rev}, were interpolated from single-channel current amplitudes and whole-vacuole tail currents (for details on the ionic conditions used see Table 2 and legends of Figs. 3 and 4A). The analysis of the various permeable ion species revealed a permeability sequence of $K^+ > TEA^+ > Cl^- > Ca^{2+} \approx Gluc^-$ listed in Table 3, whereas Mg^{2+}, $Tris^+$ and Mes^- did not significantly contribute to SV-type currents (cf. *Appendix*). This selectivity sequence and Fig. 3C indicated that in physiological conditions the SV-type conductance is based on K^+, Ca^{2+} and Cl^- fluxes between the vacuolar lumen and the cytosol. Consequently, as shown in Fig. 4A, the vacuolar outward currents, which were elicited negative to the K^+ and positive to the Cl^- equilibrium potentials of 107 and -69 mV, clearly indicated that SV-type channels are capable of releasing *both* K^+ *and* Cl^- ions from the vacuolar lumen into the cytosol. Note, however, that the deficiency of vacuolar monovalent cations in favour of a high vacuolar Ca^{2+} concentration increased the Ca^{2+} permeability of the SV-type channel (Fig. 3A; cf. Ward and Schroeder 1994).

While the orientation of the KCl gradient neither affected the selectivity nor the slow kinetics of the outward rectifier (cf. Table 2; Figs. 3C, 4A, Inset), the single-channel conductance drastically changed (Fig. 4B, C). Lowering the KCl concentration in the bath from 200 to 2 mM reduced the current amplitude of the SV-type channel from 280 to 81 ± 9 pS (Fig. 4B; $n = 3$). Together with the 80 pS-conductance a 40 pS-channel (Fig. 4C) with identical ion permeability (possibly a substate of the SV-type channel) was observed.

When on the cytosolic side 100 mM KCl was substituted by K-gluconate or TEACl, tail currents reversed at -5 ± 1.7 mV ($n = 3$, Fig. 3D) and 12.6 ± 1.5 mV ($n = 3$), as presented in Table 2. Simultaneously, the steady-state currents were reduced to 10–30% (Inset of Fig. 3D). As summarized in Tables 2 and 3, these experiments indicated that even the large, so-called 'impermeable' ions TEA^+ and $Gluc^-$ do permeate the SV-type channel. Previous results on sugar beet vacuoles showed that even millimolar additions of charged amino acids, but not neutral ones, reduced SV-type currents (data not shown; R. Hedrich and S. Marx, unpublished). Consequently, it is impossible to apply these large ions to study SV-channel selectivity under biionic conditions.

Single-channel conductance and channel density. To further elucidate the lack of ion specificity indicated in Tables 2 and 3 we attempted to saturate the conductance of single SV-type channels with increasing KCl concentration (Fig. 5). Slope conductances calculated from the linear current/voltage relation of single-channel amplitudes under symmetrical ionic conditions were determined in the range of 0.01 to 1 M KCl concentrations (in bath and pipette). The conductance of single SV-type channels linearly increased in the range of physiological KCl concentration (80–900 mM; Humble and Raschke 1971; Speer and Kaiser 1991) with a slope of 1.40 $nS \cdot M^{-1}$ in guard cells compared to 0.69 $nS \cdot M^{-1}$ in sugar beets. Guard-cell SV-type channels had a 2- to 2.5-fold higher single-channel conductance compared to the beet channel and did not saturate even at 1 M KCl. This lack of saturation demonstrated that ion permeation through the channel was not limited by anionic or cationic binding sites within the channel pore.

In order to compare the vacuolar SV-type channel density in both cell types, channel numbers per membrane area were estimated from single-channel and tail-current amplitudes. In whole vacuoles, guard-cell capacities (c) of 4–16 pF, assuming a specific membrane capacity of

Table 2. Transmembrane ion distributions, corresponding reversal potentials of SV-type currents U_{rev} and variables α to ε required for determination of permeability ratios (see text and *Appendix*)

	$[K]_o$ (mM)	$[K]_i$ (mM)	$[Cl]_o$ (mM)	$[Cl]_i$ (mM)	$[Ca]_o$ (mM)	$[Ca]_i$ (mM)	$[TEA]_o$ (mM)	$[TEA]_i$ (mM)	$[Gluc]_o$ (mM)	$[Gluc]_i$ (mM)	α	β	γ	δ	ε	U_{rev} (mV)	U'_{rev}* (mV)
1	200	2	212	14	1	1	0	0	0	0	194.0	− 617.8	− 7.9	0.0	0.0	28	30
											193.8	− 642.9	− 8.4	0.0	0.0	29	
											192.1	− 816.1	− 11.7	0.0	0.0	35	
											194.0	− 617.8	− 7.9	0.0	0.0	28	
2	200	0	212	12	1	1	0	0	0	0	200.0	− 691.1	− 8.9	0.0	0.0	30	31
3	20	200	32	212	1	1	0	0	0	0	− 52.6	200.4	2.5	0.0	0.0	− 26	− 25
											− 52.6	200.4	2.5	0.0	0.0	− 26	
											− 56.9	199.7	2.5	0.0	0.0	− 24.5	
4	100	100	121	101.2	10	0.1	0	0	0	0	0.0	− 20	19.8	0.0	0.0	0	− 1
											3.8	− 15.4	20.2	0.0	0.0	− 1	
											3.8	− 15.4	20.2	0.0	0.0	− 1	
5	150	150	170	160	5	0.1	0	0	0	0	0.0	− 10	9.8	0.0	0.0	0	0
											0.0	− 10	9.8	0.0	0.0	0	
6	100	0	112	112	1	1	0	100	0	0	100.0	− 81.3	− 2.9	− 172.6	0.0	14	13
											100.0	− 60.0	− 2.1	− 153.6	0.0	11	
											100.0	− 74.0	− 2.6	− 166.0	0.0	13	
7	100	100	112	12	1	1	0	0	0	100	14.4	− 83.82	0.6	0.0	100.0	− 4	− 5
											14.4	− 83.82	0.6	0.0	100.0	− 4	
											20.9	− 76.63	0.8	0.0	100.0	− 6	

* U'_{rev}-values were predicted from Eq. 23 using the fitted permeability ratios $P_K = 1$, $P_{Cl} = 0.28$, $P_{Ca} = 0.1$, $P_{TEA} = 0.48$ and $P_{Gluc} = 0.06$ which in turn were determined by the variables α, β, γ, δ and ε as outlined in the *Appendix*

Table 3. Ion permeability of the guard-cell SV-type channel. Relative permeability ratios (± SE) were derived from the assumptions of the constant field theory under seven different transmembrane ion gradients as outlined in the Appendix (Goldman 1943; Lewis 1979). In order to compare the channel permeability for K^+, Ca^{2+} and Cl^- with those for TEA^+ and $Gluc^-$, all permeability coefficients were calculated from concentrations rather than activites. Errors introduced by this procedure are, however, small, since the determination of P_K, P_{Cl} and P_{Ca} using the activity coefficients for K^+, Cl^- and Ca^{2+} (Robinson and Stokes 1959) resulted in $P_K = 1$, $P_{Cl} = 0.28 \pm 0.01$ and $P_{Ca} = 0.05 \pm 0.32$, values very similar to those determined below

	$X = K^+$	$X = TEA^+$	$X = Cl^-$	$X = Gluc^-$	$X = Ca^{2+}$
P_X/P_{K^+}	1.00 $n = 19$	0.48 ± 0.04 $n = 3$	0.28 ± 0.01 $n = 19$	0.06 ± 0.07 $n = 3$	0.1 ± 0.29 $n = 19$

1 μF·cm^{-2}, allowed us to calculate a minimum surface density in the range of 0.37 ± 0.08 channels μm^{-2} in guard cells ($n = 4$) compared to about 0.16 μm^{-2} in sugar beet (20 pF ≤ c ≤ 40 pF; cf. Coyaud et al. 1987). Therefore the 3.3- to 6-fold higher SV-current density of guard-cell vacuoles (7.4 ± 2.1 μA·cm^{-2}; $n = 3$; data not shown) might be well suited to mediate the large and rapid vacuolar K^+ and Cl^- fluxes during stomatal closure.

Calcium ions modulate the voltage dependence of SV-type channels. In previous studies (Hedrich and Neher 1987; Colombo et al. 1989) it was shown that SV-type currents of sugar beet and *Acer* vacuoles were under control of the cytoplasmic Ca^{2+} concentration. When this divalent cation was removed from the cytoplasmic side of guard-cell vacuoles using EGTA buffers, the guard-cell SV-type channel activity decayed (Fig. 6A), indicating the requirement of Ca^{2+} for the activation process in this type of vacuole, too. In order to specify the Ca^{2+} dependence of channel activities, the Ca^{2+} concentration in the bath was raised from nominally 0 (2 mM EGTA, no Ca^{2+} added) up to 10 mM $CaCl_2$. Although this wide concentration range exceeds the Ca^{2+} resting level by five orders of magnitude[3], it included the Ca^{2+} concentrations which have to be expected in the immediate environment of the vacuolar membrane surface during Ca^{2+} transients caused by vacuolar Ca^{2+} release and which, consequently, might be detected by SV-type channels.

Beyond these conditions the single-channel properties were analysed with respect to the unitary conductance and voltage-dependent gating. Measurements in all test solutions were alternated with measurements in 0.1 mM Ca^{2+} (control) and measurements at all test potentials with measurements at 40 mV in 30- to 60-s intervals (Fig. 6). Channel activities were corrected with respect to this internal standard. Figure 6B illustrates that the increase in Ca^{2+} concentration from 0.1 to 1 mM shifted the

[3] As in animal cells the cytosolic Ca^{2+} bulk concentrations of plant cells are as low as 0.1 to 1 μM at rest and transiently increase in the bulk to 10 μM (Miller and Sanders 1987; Felle 1991; Hille 1992). However, in further analogy to neuronal cells, during Ca^{2+} transients the free Ca^{2+} concentration in the immediate neighbourhood of open Ca^{2+} channels might rise by several hundred micromolar up to 1 mM (Llinás et al. 1991, and Roberts et al. 1990; cf. *Discussion*)

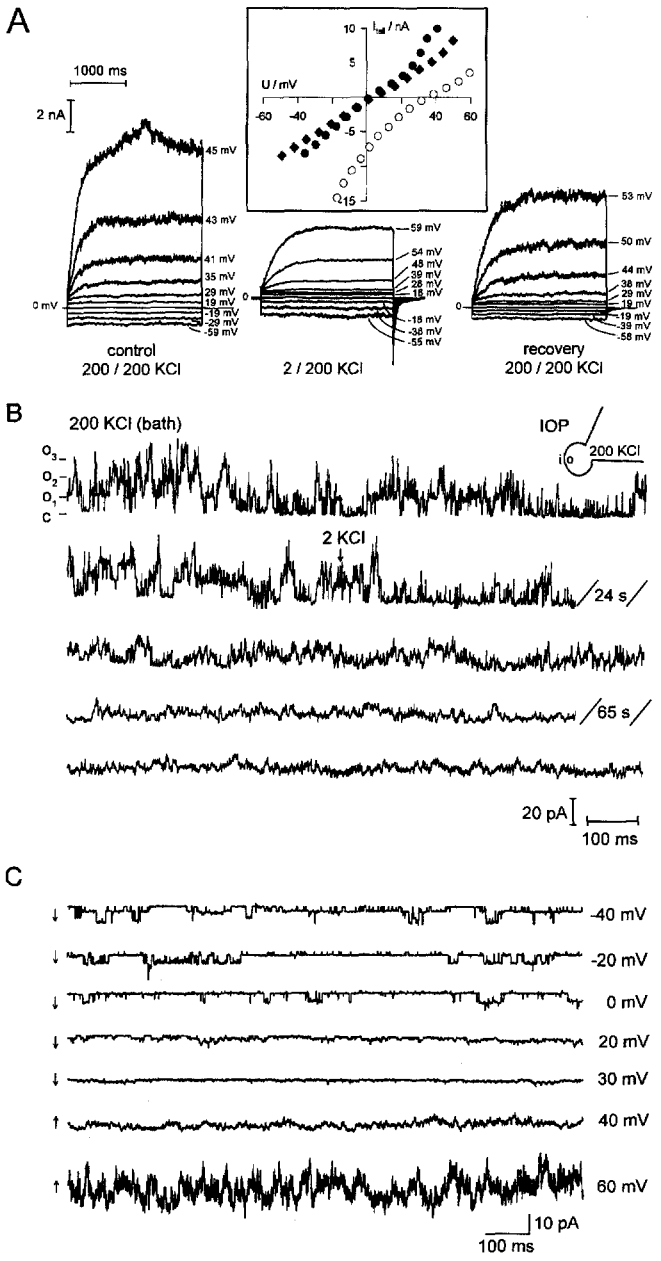

Fig. 4A–C. Vacuolar Cl^- and K^+ release mediated by SV-type channels. The pipette solution contained 200 mM KCl. **A** Depolarizing single voltage pulses elicited SV-type currents in a whole vacuole exposed to 200 mM (*control, recovery*) and 2 mM KCl concentration in the bath, respectively. In consideration of the Nernst potentials at 2 mM cytosolic KCl concentration ($E_K = 107$ mV and $E_{Cl} = -69$ mV; $E_{Ca} = 0$ mV), the positive SV-type net-currents were mainly carried by simultaneous K^+ and Cl^- fluxes into the cytosol (bath). The relative contributions of both components (the negative K^+ current and the positive Cl^- current) to the positive SV-type net currents correspond to the driving forces of the individual ions. *Inset:* Corresponding tail current/voltage relation of the vacuole shown in **C**. ●, control; ○, 2/200 mM KCl; ◆, recovery. Under symmetrical ionic conditions (control and recovery) tail currents reversed at 0 mV, whereas in 2/200 mM KCl the reversal potential shifted to 35 mV. **B** Time-dependent reduction of the single-channel conductance from 280 to 80 pS during the decrease in cytosolic KCl concentration from 200 to 2 mM. Single-channel fluctuations recorded from an inside-out patch clamped at 40 mV excised from the same cell as in **A**. **C** Voltage dependence of the SV-type channel at a reduced (2 mM) cytosolic KCl concentration. In addition to the 80 pS-conductance of the SV-type channel a 40 pS-channel was observed

threshold potential of SV-type current activation by about 20 mV, whereas 10 mM Ca^{2+} even moved the activation threshold by about 70 mV towards more-negative membrane potentials. The unitary conductance of the SV-type channel, however, was not significantly affected by Ca^{2+} changes (Fig. 6C). Since even the whole-vacuole currents activated by 0.1 mM cytoplasmic Ca^{2+} were very small (data not shown), single-channel analyses at lower Ca^{2+} concentrations were not performed.

In contrast to Ca^{2+}, cytoplasmic Ba^{2+} was not capable of activating Ca^{2+}-dependent SV-type currents in guard-cell vacuoles. Replacement of 1 mM Ca^{2+} by up to 30 mM Ba^{2+} reduced SV-type currents within 3 min almost completely (by 80–100%; Fig. 7; $n = 3$). Similar to the side-specific Ba^{2+} sensitivity of the sugar beet channel (Hedrich and Kurkdjian 1988), this finding is in contrast to the properties expected from Ca^{2+}-induced Ca^{2+} channels (Pantoja et al. 1992a; Ward and Schroeder 1994).

Channel modulation by protons. Besides Ca^{2+}, pH changes also alter the activity of different plasma-membrane channels, e.g. the guard-cell K^+ channels of *Vicia faba* (Blatt 1992; Ilan et al. 1994). In order to determine whether cytoplasmic protons are involved in the modulation of vacuolar ion fluxes, single-channel recordings were performed on inside-out patches at different pH values in analogy to the Ca^{2+} experiments (shown above). When the pH of the bathing solution was changed in the range between 8.3 and 5.3 the unitary conductance of the SV-type channel remained unaffected, whereas unspecific "run down" effects prevented the study and analysis of the channel activity at pH 8.3 and 5.3 (Fig. 8B). However, decreasing the cytoplasmic pH from 7.3 to 6.3 shifted the activation threshold by about 20 mV towards more-depolarized potentials (Fig. 8A). The sugar beet channel showed a more-complete recovery of activity with respect to pH alterations than the guard-cell homologue. In the former, we were able to vary the cytoplasmic pH between

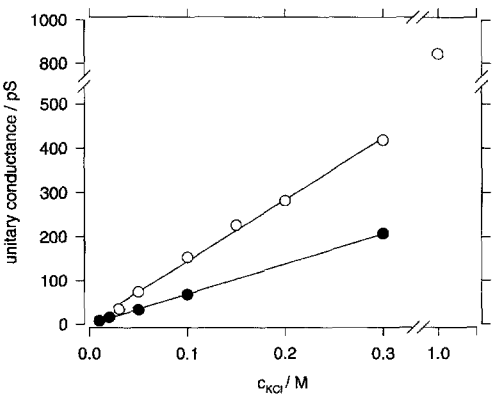

Fig. 5. Single-channel conductances of the *V. faba* guard-cell and sugar beet SV-type channels as a function of KCl concentration. Slope conductances of the single SV-type channels were 1.4 $nS \cdot M^{-1}$ and 0.69 $nS \cdot M^{-1}$ for guard cells (○) and sugar beet (●). Conductances were determined under symmetrical ionic conditions in the presence of 1 mM $CaCl_2$. Note, that in both vacuole types the SV-type conductance did not saturate in the physiological range of cytoplasmic KCl concentration

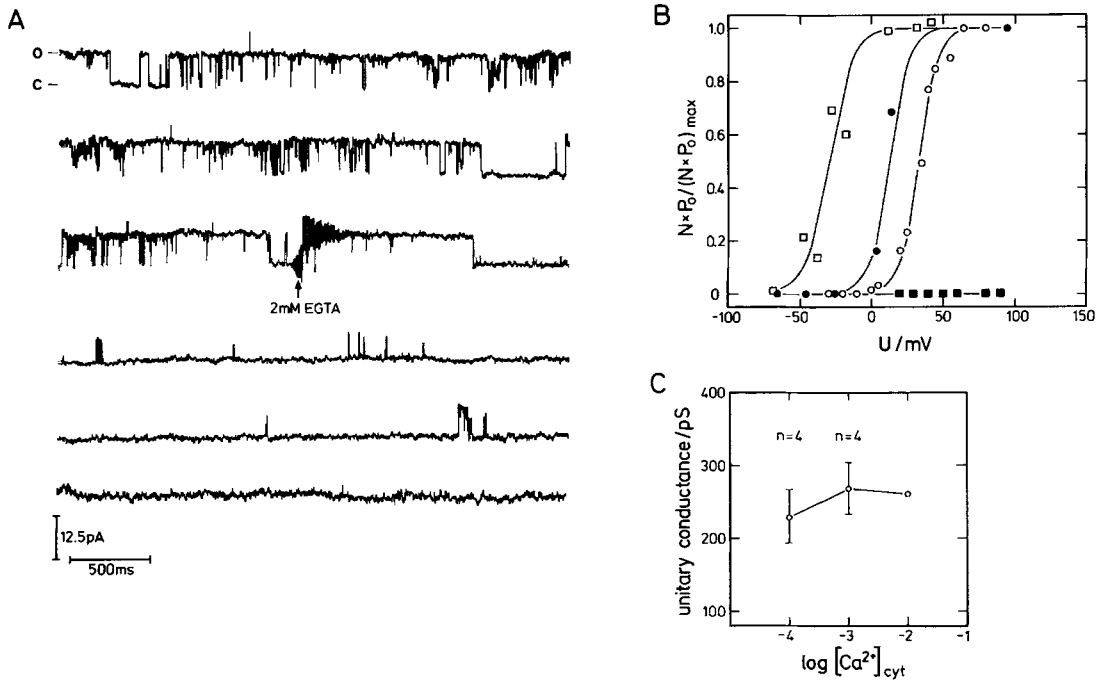

Fig. 6A–C. Calcium dependence of the guard-cell channel. **A** Single-channel currents recorded from an inside-out patch at a holding potential of 50 mV. Initially the patch was exposed to symmetrical ionic conditions in bath and pipette (200 mM KCl, 0.1 mM $CaCl_2$, 5 mM $MgCl_2$, buffered to pH 7.5). When the cytosolic free Ca^{2+} concentration was reduced upon perfusion with an EGTA-buffered (2 mM), Ca^{2+}-free bath solution (↑), the channel activity decreased. Finally, in the absence of cytoplasmic Ca^{2+}, no channel openings were observed. **B** Calcium and voltage dependence of the channel activity. Increasing the extravacuolar Ca^{2+} concentration from 0.1 (○), to 1 (●) and 10 mM $CaCl_2$ (□) shifted the threshold potential of channel opening towards negative membrane potentials while 2 mM EGTA (■) suppressed channel opening. All data were obtained from single-channel recordings of the same inside-out patch. **C** Unitary conductances of the SV-type channel at Ca^{2+} concentrations indicated in **B**. Note that Ca^{2+} changes did not affect significantly the unit conductance. Data points represent the mean ± SSD of one (in 0.1 and 1 mM $CaCl_2$) and two experiments (10 mM $CaCl_2$)

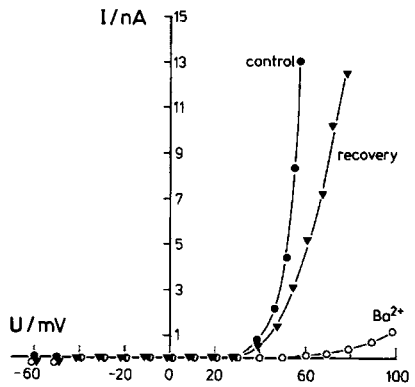

Fig. 7. Lack of SV-type channel activation by cytoplasmic Ba^{2+}. Guard-cell SV-type currents before, (●), during (○) and after (▼) exposure to 30 mM Ba^{2+}. Application of even 30-fold higher Ba^{2+} concentration than those used for Ca^{2+} activation of SV-type channels, could not replace the Ca^{2+}

3.8 and 8.8 with repetitive measurements at pH 7.8 (control pH) in between. As in guard cells, the increase in cytoplasmic proton concentration decreased the channel activity rather than the unitary conductance (Figs. 8 and 9, open circles). The proton inhibition curve of the SV-type channel could be described by the Hill equation with an apparent pK_d of 6.8 and a Hill coefficient of $n^H_{app} = 0.76$ (with a correlation coefficient of $r = 0.9999$), indicating no positive cooperativity in proton binding on the channel protein (Fig. 9A).

In the following we elucidated whether the channel is modulated by protons and Ca^{2+} in a side-specific manner. Within the range of physiological Ca^{2+} concentration found in vacuoles (0.1–10 mM; Macklon 1984; Hepler and Wayne 1985) modulation of neither guard-cell nor sugar beet SV-type channels was observed (data not shown). In a similar series of experiments the effect of vacuolar protons on the single-channel properties was studied on outside-out patches of sugar beet vacuoles (Fig. 9B, C). At a holding potential of 60 mV[4], the vacuolar proton concentration was stepped from pH 7.8 to 3.8, alternating with steps to the assumed physiological pH of 5.8 in between. Channel activities were normalized with respect to pH 5.8. Neither vacuolar nor cytoplasmic protons altered the unitary conductance of the channel (Fig. 9C). The pH changes in the vacuole, however, caused reductions in channel activity by 7%, 12% and up to 66%, when the vacuolar pH was decreased from 7.8 to 6.8, from pH 6.8 to 5.8, and from pH 5.8 to 4.8 (Fig. 9B,

[4] The channel properties analyzed at 60 mV resembled those at more-depolarized potentials, at least qualitatively

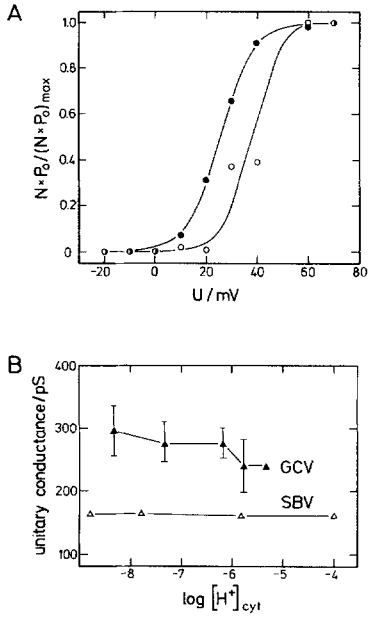

Fig. 8A, B. pH dependence of the voltage-gated SV-type channels in guard cells. **A** Decreasing the cytoplasmic pH from 7.3 (●) to 6.3 (○) shifted the voltage threshold of channel activation by 20 mV towards more positive membrane potentials. Data points represent the mean channel activities recorded from two different inside-out patches. **B** Unitary conductances of the SV-type channel in guard cells (*GCV*, ▲) and sugar beet vacuoles (*SBV*, △) in response to changes in the cytoplasmic pH. Note that the unit conductances of both cell types remained unaffected. Pipette solutions were buffered to pH 7.3 in the guard-cell experiments and to pH 5.8 for measurements on sugar beet vacuoles. The unitary conductance of the sugar beet channel was determined with 200 mM KCl, 1 mM $CaCl_2$, 5 mM $MgCl_2$, 10 mM citrate/KOH in bath and pipette solution

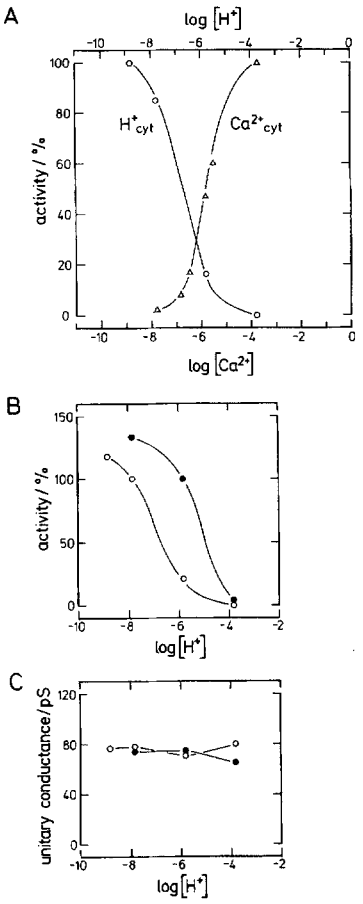

Fig. 9A–C. Reciprocal modulation of SV-type currents by cytoplasmic protons and Ca^{2+} in sugar beet vacuoles. **A** Increasing the cytoplasmic proton concentration from pH 8.8 to 3.8 caused a complete inhibition of channel activity (○) at 40 mV, whereas a rise in cytoplasmic calcium concentration from $1.48 \cdot 10^{-8}$ to 10^{-4} M increased the activity (△; Hedrich and Neher 1987). **B** Modulation of the single-channel activity by the vacuolar (●) and cytoplasmic pH (○) recorded from outside-out and inside-out patches of sugar beet vacuoles clamped at 60 mV and 40 mV, respectively. Corresponding to the physiological proton concentration, channel activities were normalized to pH 5.8 (vacuole) and 7.8 (cytosol). Bath and pipette solutions contained 100 mM KCl, 1 mM $CaCl_2$, 5 mM $MgCl_2$, 10 mM citrate / KOH. Pipette solutions were buffered to pH 7.8 (outside-out) and pH 5.8 (inside-out). **C** The unitary conductance was neither affected by vacuolar (●) nor cytoplasmic (○) pH changes

filled circles). Similar titration curve analysis yielded an apparent dissociation constant pK_s of ≈ 5 compared to 6.8 for modulation by cytoplasmic protons (Fig. 9B, open circles). Thus an asymmetry in the channel structure might explain the 100-fold decreased channel sensitivity to vacuolar protons. These results suggest at least two independent proton-binding sites or access pathways on the cytoplasmic and vacuolar membrane face of the SV-type channel.

Calmodulin antagonists and inhibitors. As in animal cells, many Ca^{2+}-induced processes in plants are amplified by Ca^{2+}-binding proteins like cytoplasmic or membrane-associated CaMs (Evans et al. 1991). Calmodulin and structurally different CaM antagonists were thus applied to the cytoplasmic face of the guard-cell SV-type channel to elucidate the role of CaM in the Ca^{2+}- and voltage-dependent activation process. In the presence of the Ca^{2+}-binding protein, however, vacuolar currents could not be enhanced by cytoplasmic application of 1 μM exogenous CaM from wheat germ ($n = 4$), bovine hearts ($n = 2$) or spinach ($n = 4$). On the other hand, the naphthalenesulfonamide derivative W-7, known to inhibit the plant plasma-membrane Ca^{2+}-ATPase (Gilroy et al. 1987), elicited a flickering block. This response might indicate an interaction of the inhibitor with the open mouth of the SV-type channel (Fig. 10). In the concentration range of 1–100 μM, W-7 evoked a reversible and dose-dependent inhibition of channel activity with an apparent 50%-inhibition constant, $K_i \approx 4$ μM ($n = 3$, Fig. 10B). With increasing cytoplasmic inhibitor concentration the mean open time strongly decreased whereas the single-channel conductance remained unaffected (Fig. 10C). Because of the lipophilic character of W-7, we could not exclude the possibility that the inhibitor entered vacuolar sites by diffusion across the bilayer. Thus the side specificity of W-7 was determined by application of the CaM antagonist directly to the vacuolar membrane side using the outside-out configuration (vacuolar side of the membrane exposed to the bath). With 10 μM W-7 in the bath,

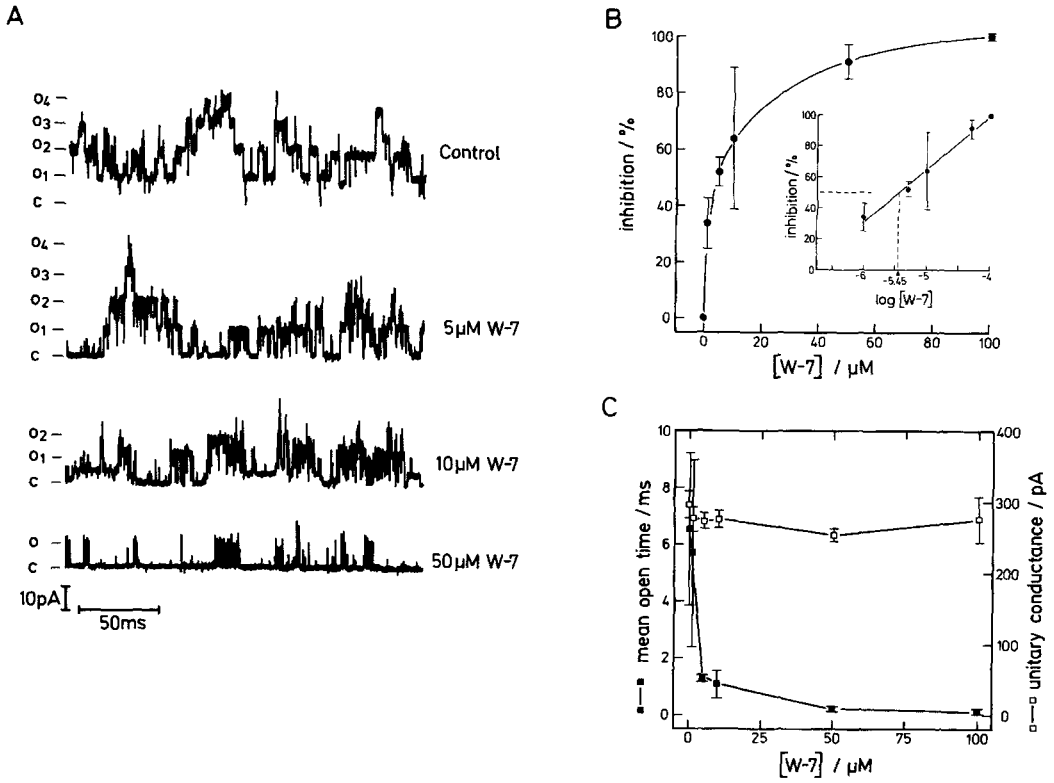

Fig. 10A–C. Inhibition of the SV-type channel in guard cells by the CaM antagonist W-7. **A** SV-type channels in an inside-out membrane patch held at 40 mV. The increase in the cytosolic W-7 concentration evoked a flickering channel block. Current traces were filtered at 5 kHz and analysed with a sampling frequency of 25 kHz. **B** Dependence of the single-channel inhibition as a function of blocker concentration. Inhibition of the channel activity was determined 3 min after incubation with W-7. The dose-response curve was fitted by eye. Linear regression analysis of the semi-logarithmic plot (*Inset*) revealed a half-maximal inhibition at 4 μM. **C** W-7 evoked a dose-dependent decrease in the mean open time (■) without changing significantly the single-channel conductance (□). Data points in **B** and **C** were obtained from three different cells. Each experiment was based on at least three exposures to different W-7 concentrations with control measurements at 30 mV or 40 mV in between

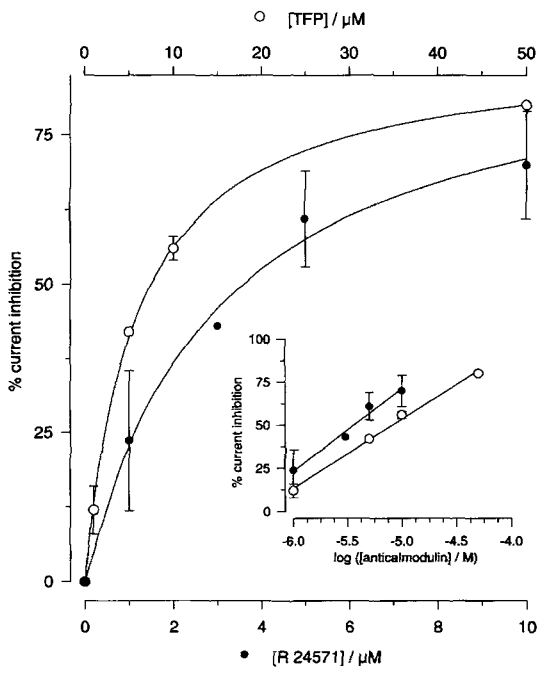

flickering channel block was delayed by about 2 min ($n = 3$, data not shown) compared to cytoplasmic application, pointing to a more cytoplasm-orientated perception site. In contrast to W-7 and to their known function as anti-CaMs, R 24571 and TFP both evoked an irreversible channel block when applied to the cytoplasmic membrane side of whole vacuoles. Dose dependencies of channel block by W-7, TFP and R 24571 were determined after 3 min incubation time in the inhibitor solution. The current inhibition by R 24571 and TFP was determined by single-voltage-pulse experiments stepping the membrane potential from 0 to 100 mV. As shown in Fig. 11, both inhibitors evoked a dose-dependent channel inhibition

Fig. 11 Dose dependence of SV-current inhibition in guard-cell vacuoles by the anti-calmodulins R 24571 and TFP. Irreversible block of whole-vacuolar SV-type currents was determined by single 2.5-s voltage pulses from a holding of 0 mV to 100 mV 3 min after inhibitor application on the cytosolic side of the vacuoles. Dose-reponse curves of R 24571 (●) and TFP (○) were fitted by eye. Each data point represents the mean ± SSD of three independent experiments. *Inset*: Linear regression of the semilogarithmic data plot revealed the inhibition constants of 4 and 8 μM for R 24571 and TFP, respectively

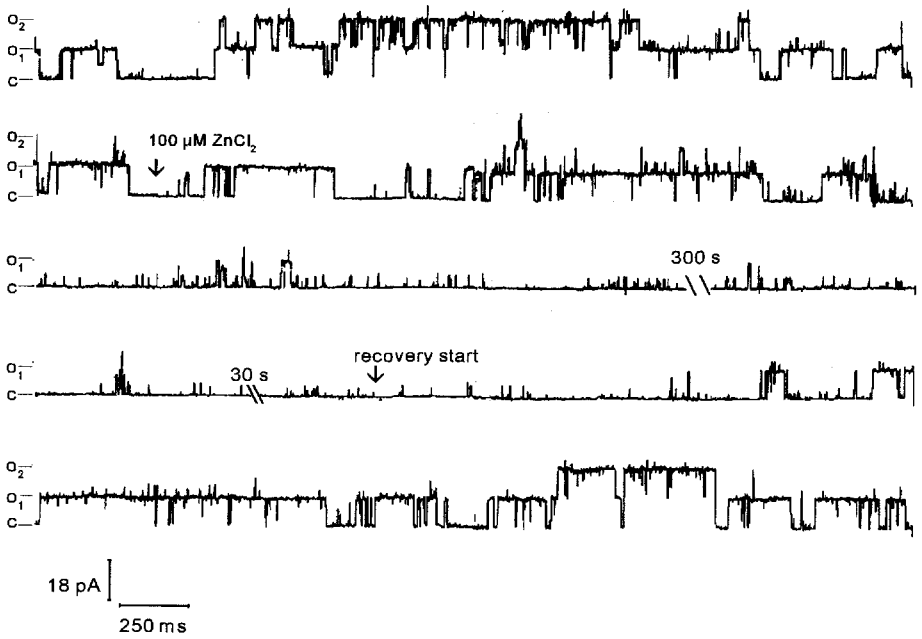

Fig. 12. Reversible Zn^{2+} block of single guard-cell SV-type channels. Representative single-channel fluctuations before, during and after application of 100 μM $ZnCl_2$ recorded from an inside-out patch at 50 mV. *Arrows* indicate the initiation and termination of chamber perfusion with $ZnCl_2$

with apparent $K_{i(R\,24571)}$ and $K_{i(TFP)}$ of 4 μM and 8 μM, respectively. In contrast to W-7, these two CaM antagonists did not elicit a flickering channel block in single-channel experiments (data not shown). Thus their sites of interaction might be different from those for W-7.

In order to compare common features of the two SV-channel types, in addition to voltage-, Ca^{2+}- and pH-modulation their susceptibility to anion-transport inhibitors was investigated. In previous studies characterizing the pharmacology of the SV-type channel in sugar beet vacuoles (Hedrich and Kurkdjian 1988), DIDS and Zn^{2+} were potent cytosolic inhibitors. In contrast to the sugar beet channel, DIDS did not block guard-cell SV-type channels even at 100 μM concentration to the cytosolic side ($n = 5$), in line with observations on the SV-channel equivalent of suspension-cultured sugar beet cells (Pantoja et al. 1989). Thus, DIDS-inhibition of SV-type channels may be tissue specific or may be restricted to a particular developmental state. In agreement with the findings on sugar beet and radish taproots (Hedrich and Kurkdjian 1988; Alexandre et al. 1990), 100 μM Zn^{2+} applied from the cytoplasmic membrane side almost completely ($\geq 95\%$) reduced the channel activity within 10–30 s whereas the unitary conductance remained constant (Fig. 12, $n = 4$).

Discussion

Consequences of the lack of ion specificity. Reversal potentials of the SV-type channels could be successfully predicted by the relative ion permabilities $P_K = 1$, $P_{Cl} \approx 0.28$ and $P_{Ca} \approx 0.1$ determined by assuming independent ion movement (Tables 2, 3; Figs. 3B–D, 4A). In contrast to Ward and Schroeder (1994; cf. Table 1), in our study the relative permeability coefficients were determined under physiologically relevant transmembrane K^+, Cl^- and Ca^{2+} gradients[5]. In the presence of Ca^{2+} as the exclusive permeable cation in the lumen (10 mM versus 0.1 mM in the cytoplasm; Fig. 3A), using Eq. 23 (see Appendix) and the permeability ratios outlined above, one would expect a reversal potential of −18 mV instead of 60 mV. In analogy, under the experimental conditions used by Ward and Schroeder (1994)[6] one would anticipate that SV-type currents will reverse at −27 mV rather than at 14 mV. Obviously, under these conditions the predicted Ca^{2+} permeability strongly differs from the experimental results. When, however, K^+ concentrations as low as 20 mM were added to the vacuolar side, representing a fraction of the in-vivo concentration only, the permeability of the channel was dominated by K^+ and Cl^-, and did not change significantly upon an increase to 212 mM (cf. Table 2). These results indicate that permeable monovalent cations such as K^+ at the vacuolar membrane side may prevent alteration of the selectivity filter. For example, Ca^{2+} binding to the conductive pore might reduce the permeation of K^+ and Cl^- in favour of Ca^{2+} ions. Since the direction and amplitudes of ion fluxes through the pore(s) are determined by the electrochemical potential for each ion species permeating the channel, SV-type currents might present the net current amplitudes constituted by K^+, Cl^- and small Ca^{2+} currents (cf. Fig. 4). The fact that the single-channel conductance of SV-type channels lacks saturation up to 1 M KCl (Fig. 5)

[5] K^+ concentrations of 100–900 mM in the vacuole and around 80–100 mM in the cytosol were described for guard cells (Humble and Raschke 1971; Penny and Bowling 1974; MacRobbie 1988). Cl^- concentrations were expected to range between 1–280 mM (vacuole) and 5–100 mM (cytosol; Speer and Kaiser 1991). With respect to physiological Ca^{2+} concentrations, please, cf. footnote 3

[6] i.e. 50 mM $CaCl_2$ and 5 mM Mes/Tris pH 5.5 in the vacuolar lumen and 100 mM KCl, 5 mM $CaCl_2$, 10 mM Tris/Mes on the cytosolic side of the membrane

further supports the K^+ and Cl^- permeability of the pore(s). Characterization of the channel selectivity in the presence of large cations or anions (TEA^+, $Gluc^-$) might indicate that under these conditions cation and anion movements are not independent (Fig. 3D). When they permeated the channel, $Gluc^-$ and TEA^+ reduced the current amplitude, a result which suggests that both ions impeded the permeation of K^+, Cl^- and Ca^{2+}. These observations are in line with previous findings of Pantoja et al. (1992b), who came to a different conclusion[7]: When varying amounts K-gluconate were added to keep the cytosolic K^+ concentration constant on both sides of the membrane, but to decrease the Cl^- concentration in favour of $Gluc^-$ in the bath, SV-type currents decreased.

Calcium and protons affect gating. The identification of gating modification by cytosolic Ca^{2+} and protons shown here might help to understand channel function in vivo. Cytosolic Ca^{2+} ions affected the voltage-dependent channel activity without changing the unitary conductance in guard cells (Fig. 6), in line with previous results on SV-type currents in sugar beet (Hedrich and Neher 1987) or barley aleurone (Bethke and Jones 1994). However, in guard-cell vacuoles, activation by the bivalent cation required concentrations of at least 100 μM (Fig. 6), a Ca^{2+}-sensitivity similar to that of mammalian "maxi"-K(Ca) channels coded by the gene *mSlo* (Butler et al. 1993). Upon Ca^{2+} entry into the cytosol through voltage-dependent Ca^{2+} channels, the local free calcium concentration on the cytoplasmic surface of animal plasma membranes increased to several hundred micromolar (Roberts et al. 1990; Llinás et al. 1991) with respect to an averaged bulk concentration of 5 μM. In analogy, the observed Ca^{2+}-sensitivity of guard-cell SV-type channels could point to the local free calcium concentration at the cytoplasmic surface of the vacuolar membrane during Ca^{2+} release through vacuolar Ca^{2+} channels (Johannes et al. 1992; Allen and Sanders 1994a). Since all experiments were performed against a background of high ionic strength and bivalent cation concentration (200 mM KCl and 5 mM $MgCl_2$) and considering that Ba^{2+}, even applied at 30-fold higher concentrations, could not substitute for Ca^{2+} to activate SV-type channels (Fig. 7), we suggest a Ca^{2+}- and pH-specific channel gating rather than a surface charge effect. Therefore, we propose a regulatory Ca^{2+} binding site on the cytoplasmic face of the channel capable of modifying the voltage sensor.

In addition, we could show that cytoplasmic protons elicit the down-regulation of channel activity in storage-cell and guard-cell vacuoles, shifting the working range of the SV-type channel towards depolarizing membrane potentials (Figs. 8, 9A, B). Small variations of cytosolic pH which correspond to the physiological bandwidth of H^+ activity ($6.8 \leq pH_{cyt} \leq 7.7$; Felle 1988a; Tarczynski and Outlaw 1990; Blatt and Armstrong 1993) evoked large changes in channel activity (Fig. 9). Similar to the mutant I369H of the animal voltage-dependent K channel Kv2.1 (DeBiasi et al. 1993), the cytosolic proton blockade of the SV-type channel ($pK_a \approx 6.8$) was consistent with the pK_a of histidine in aqueous solution. Likewise, SV-type currents in both plant tissues showed a pronounced reversible Zn^{2+} block (Fig. 12; cf. Hedrich and Kurkdjian 1988). Since both protons and Zn^{2+} are known to interact with imidazole side-chains, these results might point to a histidine residue exposed to the cytosolic mouth of the SV-type channel pore. Whether or not cytosolic protons, Zn^{2+} and Ca^{2+} ions compete for a common binding side requires further elucidation. The Ca^{2+}- and H^+-dependent modulation of voltage-dependent SV-type channels, steepest around the resting level of both ions (Fig. 9), will, upon changes in the concentration of one ion relative to the other, strongly affect the open probability of the channel.

Furthermore, small changes in the physiological pH range of vacuoles ($3.8 \leq pH_{vac} \leq 6$; Felle 1988b; Yin et al. 1990; Siebke et al. 1992) altered the channel activity as well (Fig. 9B). Since low vacuolar pH values accompany an increase in vacuolar anion content, proton inhibition of SV-type channels might allow plant cells to down-regulate ion influx into the cytosol in the presence of a steep gradient (negative feedback). A similar flux control has very recently been observed for GCAC1, a *g*uard *c*ell plasma membrane *a*nion *c*hannel (Hedrich and Marten 1993; Hedrich et al. 1994). Such a control mechanism might play a vital role in plants exhibiting crassulacean acid metabolism or in guard cells, both of which are characterized by diurnal oscillations and transients in vacuolar ion content.

Is CaM a modulator of SV-type channels? Although participation of CaM in channel activation has previously been shown in different animal organisms, its involvement in plant vacuolar channel physiology has just emerged (Weiser et al. 1991; Bethke and Jones 1994). In this study a dose-dependent inhibition of SV-type channels was caused by three different CaM antagonists, W-7, TFP and R24571 (Fig. 10B, 11). Only the block of W-7 was reversible and characterized by flickering transitions between the open and a non-conducting state of the channel (Fig. 10A, C). Thus different inhibitor-binding sites on the channel protein or channel-associated CaM might exist. Our findings, like those of Weiser et al. (1991), however, do not exclude the possibility that the inhibitors act in a CaM-independent manner, such as by direct binding on CaM-like domains of the protein itself (Harper et al. 1991). On the other hand, if CaM is involved in channel activation, it should be tightly bound to the channel protein, since SV-type currents could be measured without addition of exogenous CaM after vacuole isolation in EGTA-buffered, Ca^{2+}-free solution (Figs. 1–12). Whether bound CaM represents the Ca^{2+} sensor on SV-type channels or a distinct cytosolic Ca^{2+}-binding site requires further clarification.

Physiological function of the guard-cell channel. The unitary conductance of the guard-cell channel of 281 ± 20 pS by far exceeds that of SV-type channels known from other tissues (Table 4). In the vacuolar membrane of guard-cells,

[7] Since the $Gluc^-$ permeation through the SV-type channel was not taken into account, a regulatory effect of cytoplasmic Cl^- responsible for decreasing current amplitudes at decreasing Cl^- concentration in the bath was postulated

Table 4. Unitary conductances (± SD) and selectivity of SV-type channels in different plant cells/tissues

Plant	Tissue	Solution[§]	Conductance	Selectivity	Authors
Hordeum vugare	Aleurone	100 mM KCl	26 pS	$K^+ \gg Cl^-$	Bethke and Jones 1994
Beta vulgaris	Suspension culture cells	100 mM KCl	51–68 pS	$K^+ > Cl^-$	Pantoja et al. 1992a, b
Nicotiana tabaccum	Mesophyll	100 mM KCl	60–80 pS		Hedrich et al. 1988
Plantago media, *Plantago maritima*	Root cells	100 mM KCl	60–70 pS	$K^+ = Na^+ > Cl^-$	Maathuis and Prins 1991b
Beta vulgaris conditiva	Hypocotyl root	100 mM KCl	65 pS	$K^+ > Cl^-$	Alexandre et al.1990
Chenopodium rubrum	Suspension culture cells	100 mM KCl	70 pS	$K^+ > Cl^-$	Bentrup 1989
Vigna unguiculata	Stem	100 mM KCl	102 ± 4 pS	$K^+ \approx Na^+ > Cl^-$	Maathuis and Prins1991*a*
Riccia fluitans	Thallus	200 mM KCl	120–140 pS		Hedrich et al. 1988
Beta vulgaris	Taproot	200 mM KCl	120–160 pS	$K^+ = Na^+ > Ac^- > NO_3^- > mal^{2-} > Cl^-$	Hedrich and Neher1987; Schulz-Lessdorf and Hedrich, this paper
Allium cepa	Guard cells	200 mM KCl	210 ± 17 pS	$Na^+ > K^+ > Rb^+ > Cs^+ \gg Cl^-$	Adomeo and Zeiger1994
Vicia faba	Guard cells	200 mM KCl	281 ± 20 pS	$K^+ > TEA^+ > Cl^- > Ca^{2+} \approx Gluc^-$	Schulz-Lessdorf and Hedrich 1992 and this paper

* On both sides of the membrane

SV-type channels are expressed which have twice the unitary conductance and channel density of those in sugar beet taproots. In comparison to the sugar beet channel ($P_K/P_{Cl} \approx 6$; Hedrich and Neher 1987) the guard-cell channel is characterized by an even lower selectivity ($P_K/P_{Cl} \approx 3.5$; Table 3). Considering the high K^+ and Cl^- permeability, together with the physiological ion concentrations and their gradients, one might suggest that during stomatal closure guard-cell SV-type channels could mediate fast release of both anions and cations into the cytosol.

The large single-channel conductance (Fig. 2; Table 4), low selectivity (Tables 3, 4) as well as the lack of saturation (Fig. 5) implicate the requirement for a strong cellular control of SV-type channel opening. As shown here, SV-type channels behave like voltage-gated channels, modulated by second messengers such as cytosolic Ca^{2+} and pH. Cytosolic alkalinization in combination with the transient increase in cytoplasmic Ca^{2+} concentration have recently been observed after binding of abscisic acid to the plasma membrane of root-, hypocotyl- and guard cells (Gehring et al. 1990; Irving et al. 1992). Our experiments provide evidence that Ca^{2+} activation (Hedrich and Neher 1987; Colombo et al. 1989; Weiser and Bentrup 1990; Bethke and Jones 1994) and proton inhibition are common, tissue-independent features of SV-type channels in higher plants. Consequently, SV-type channels may function as a vacuolar receptor site for Ca^{2+} and protons in the control of stomatal movement. Thus, an abscisic-acid-induced increase in cytosolic Ca^{2+} and alkalinization of pH should be transduced into a vacuolar response, i.e. the activation of SV-type channels which in turn mediate anion and K^+ efflux into the cytosol (cf. MacRobbie 1988, 1990). Since SV-type channels activate at positive membrane potentials (Fig. 2C), "helper channels", e.g. inositoltrisphosphate-activated or Gd^{3+}-sensitive Ca^{2+}-release channels, have to be postulated to depolarize the negative vacuolar resting potential towards the Ca^{2+}- and proton-modulated threshold of SV-type channel activation (Alexandre et al. 1990; Sanders et al. 1990; Allen and Sanders, 1994a). Resulting K^+ and Cl^- efflux (cf. Fig. 4) would be accompanied by a Ca^{2+} release into the cytosol (cf. Table 3) which in turn could act as a secondary Ca^{2+} signal and provide for a self-propagating feed-forward activation of vacuolar SV-type channels. Via such a mechanism the vacuolar ion release could be maintained for tens of minutes and enable solute release in the time scale required for stomatal closing. Thereafter, cations (K^+) and anions may use separate pathways: Anion efflux from the cytosol into the extracellular space through voltage-dependent, Ca^{2+}- and nucleotide-modulated anion channels (Keller et al. 1989; Hedrich et al. 1990) and K^+ ions through outward-rectifying K^+_{out} channels (Schroeder et al. 1987).

Appendix

Relative permeability ratios of the SV-type channel were derived from the reversal potential and constant field assumptions. According to the general current equation for ions (Hodgkin and Katz 1949) current contributions of

K^+, Ca^{2+}, Cl^-, TEA^+, $Gluc^-$, Mg^{2+}, $Tris^+$ and Mes^- fluxes to the total current (I_{tot}) are given by the sum of the individual components (Eq. 4):

$$I_{tot} = I_K + I_{Ca} + I_{Cl} + I_{TEA} + I_{Gluc} + I_{Mg} + I_{Tris} + I_{Mes} \quad \text{(Eq. 4)}$$

Currents carried by each ion species are given by the following equations:

$$I_K = \frac{F^2 P_K U}{RT} \cdot \frac{([K^+]_o - [K^+]_i e^{FU/RT})}{1 - e^{FU/RT}} \quad \text{(Eq. 5)}$$

$$I_{Cl} = \frac{F^2 P_{Cl} U}{RT} \cdot \frac{([Cl^-]_i - [Cl^-]_o e^{FU/RT})}{1 - e^{FU/RT}} \quad \text{(Eq. 6)}$$

$$I_{Ca} = \frac{4F^2 P_{Ca} U}{RT} \cdot \frac{([Ca^{2+}]_o - [Ca^{2+}]_i e^{2FU/RT})}{1 - e^{2FU/RT}} \quad \text{(Eq. 7)}$$

$$I_{TEA} = \frac{F^2 P_{TEA} U}{RT} \cdot \frac{([TEA^+]_o - [TEA^+]_i e^{FU/RT})}{1 - e^{FU/RT}} \quad \text{(Eq. 8)}$$

$$I_{Gluc} = \frac{F^2 P_{Gluc} U}{RT} \cdot \frac{([Gluc^-]_i - [Gluc^-]_o e^{FU/RT})}{1 - e^{FU/RT}} \quad \text{(Eq. 9)}$$

$$I_{Mg} = \frac{4F^2 P_{Mg} U}{RT} \cdot \frac{([Mg^{2+}]_o - [Mg^{2+}]_i e^{2FU/RT})}{1 - e^{2FU/RT}} \quad \text{(Eq. 10)}$$

$$I_{Tris} = \frac{F^2 P_{Tris} U}{RT} \cdot \frac{([Tris^+]_o - [Tris^+]_i e^{FU/RT})}{1 - e^{FU/RT}} \quad \text{(Eq. 11)}$$

$$I_{Mes} = \frac{F^2 P_{Mes} U}{RT} \cdot \frac{([Mes^-]_i - [Mes^-]_o e^{FU/RT})}{1 - e^{FU/RT}} \quad \text{(Eq. 12)}$$

where U is the membrane potential and R, T, F have their usual physical meanings; P_X denotes the permeability coefficient for the ion X, and $[X]_o$ and $[X]_i$ its concentrations outside (lumen) and inside (cytosol) of the vacuolar membrane. Since at the reversal potential I_{total} is set equal to zero, Eq. 4 is solved with $U = U_{rev}$ using the equations (Eq. 5) to (Eq. 12) and simplified to:

$$0 = P_K \cdot \alpha + P_{Cl} \cdot \beta + P_{Ca} \cdot \gamma + P_{TEA} \cdot \delta + P_{Gluc} \cdot \varepsilon + P_{Mg} \cdot \phi + P_{Tris} \cdot \varkappa + P_{Mes} \cdot \eta \quad \text{(Eq. 13);}$$

In principle this linear equation system (Eq. 13) had to be used for fitting the free parameters P_K, P_{Cl}, P_{Ca}, P_{TEA}, P_{Gluc}, P_{Mg}, P_{Tris} and P_{Mes} in at least eight different transmembrane ion gradients, where the known variables α, β, γ, δ, ϕ, $\varkappa$ and η substitute the following terms:

$$\alpha = [K^+]_o - [K^+]_i e^{FU_{rev}/RT} \quad \text{(Eq. 14)}$$

$$\beta = [Cl^-]_i - [Cl^-]_o e^{FU_{rev}/RT} \quad \text{(Eq. 15)}$$

$$\gamma = \frac{4([Ca^{2+}]_o - [Ca^{2+}]_i e^{2FU_{rev}/RT})}{1 - e^{FU_{rev}/RT}} \quad \text{(Eq. 16)}$$

$$\delta = [TEA^+]_o - [TEA^+]_i e^{FU_{rev}/RT} \quad \text{(Eq. 17)}$$

$$\varepsilon = [Gluc^-]_i - [Gluc^-]_o e^{FU_{rev}/RT} \quad \text{(Eq. 18)}$$

$$\phi = \frac{4([Mg^{2+}]_o - [Mg^{2+}]_i e^{2FU_{rev}/RT})}{1 + e^{FU_{rev}/RT}} \quad \text{(Eq. 19)}$$

$$\varkappa = [Tris^+]_o - [Tris^+]_i e^{FU_{rev}/RT} \quad \text{(Eq. 20)}$$

$$\eta = [Mes^-]_i - [Mes^-]_o e^{FU_{rev}/RT} \quad \text{(Eq. 21)}$$

In order to minimize the number of free parameters to the relevant ones, however, the fitting procedure was started taking initially only α, β and γ into account for five different experimental conditions (cf. Table 2). In the following steps all combinations with the remaining free parameters (δ–η) were successively added to the fitting operation. In the absence of TEA^+ and $Gluc^-$ the best fits were obtained assuming that K^+, Cl^- and Ca^{2+} permeate the channel (conditions 1–5) in Table 2. In this way a significant contribution of Mg^{2+}, $Tris^+$ or Mes^- could be ruled out. However as outlined in the text, the location of the reversal potential was affected by TEA^+ and $Gluc^-$ in the bathing solution. Taking this into account Eq. 13 simplifies to the following expression (Eq. 22):

$$0 = P_K \cdot \alpha + P_{Cl} \cdot \beta + P_{Ca} \cdot \gamma + P_{TEA} \cdot \delta + P_{Gluc} \cdot \varepsilon \quad \text{(Eq. 22)}$$

By fitting the permeability coefficients of Eq. 22 under all conditions listed in Table 2 we gained the values given in Table 3.

Fit quality of the permeability coefficients was examined by comparison of the reversal potentials predicted according to the Goldmann-Hodgkin-Katz voltage equation (Eq. 23) to the U_{rev} measured under the various experimental conditions. Thereby the GHK equation was modified according to Lewis (1979) with regard to bivalent cations (C^{2+}) as well as monovalent cations (C^+) and anions (A^-) on both sides of the membrane:

$$U_{rev} = \frac{R \cdot T}{F} \cdot \ln \frac{\sum_j P_{C_j} [C^+]_o + \sum_k P_A - [A_k^-]_i + \sum_l 4P^*_{C_l^{2+}} [C^{2+}]_o}{\sum_j P_{C_j} [C^+]_i + \sum_k P_{A_k^-} [A_k^-]_o + \sum_l 4P^*_{C_l^{2+}} [C^{2+}]_i \cdot e^{FU_{rev}/RT}} \quad \text{(Eq. 23);}$$

with P_{C^+} and P_{A^-} as permeability coefficients for C^+ and A^- and $[X]_o$ and $[X]_i$ as the external and internal concentrations of the ion X. $P^*_{C^{2+}}$ is related to the permeability coefficient for the bivalent cation ($P_{C^{2+}}$) as described by Eq. 24

$$P^*_{C^{2+}} = \frac{P_{C^{2+}}}{1 + e^{FU_{rev}/RT}} \quad \text{(Eq. 24)}$$

We thank R. Benz (Institute of Biotechnology, Würzburg, Germany), F. Conti, (Istituto di cibernetica e Biofisica, Genova, Italy) and C.L. Slayman (Department of Cellular and Molecular Physiology, Yale School of Medicine, New Haven, Conn., USA) for helpful discussion of the manuscript and C. Zeilinger (Institute of Biophysics, Hannover, Germany) and G. Hinz (Institute of Plant Physiology, Göttingen, Germany) for purification of wheat-germ CaM. Studies were funded by Deutsche Forschungsgemeinschaft grants to R.H.

References

Aldrich RW, Yellen G (1983) Analysis of nonstationary channel kinetics. In: Sakmann B, Neher E (eds) Single channel recordings. Plenum Press, London, pp 287–300

Alexandre J, Lassalles JP, Kado RT (1990) Opening of Ca^{2+} channels in isolated red beet root vacuole membrane by inositol 1,4,5-trisphosphate. Nature 343: 567–570

Allen GJ, Sanders D (1994a) Two voltage-gated calcium release channels coreside in the vacuolar membrane of broad bean guard cells. Plant Cell 6: 685–694

Allen GJ, Sanders D (1994b) Osmotic stress enhances the competence of *Beta vulgaris* vacuoles to respond to inositol 1,4,5-triphosphate. Plant J 6: 687–695

Amodeo G, Zeiger E (1994) A cationic channel in the guard cell tonoplast of *Allium cepa*. Plant Physiol 105: 999–1006

Anderson JM (1983) Purification of plant calmodulin. Methods Enzymol 102: 9–16

Bentrup FW (1989) Cell physiology and membrane transport. Prog Bot 51: 70–79

Bertl A, Slayman CL (1990) Cation-selective channels in the vacuolar membrane of *Saccharomyces*: Dependence on calcium, redox state, and voltage. Proc Natl Acad Sci USA 87: 7824–7828

Bertl A, Blumwald E, Coronado R, Eisenberg R, Findlay G, Gradmann D, Hille B, Köhler K, Kolb HA, MacRobbie E, Meissner G, Miller C, Neher E, Palade P, Pantoja O, Sanders D, Schroeder J, Slayman C, Spanswick R, Walker A, Williams A (1992) Electrical measurements on endomembranes. Science 258: 873–874

Bethke PC, Jones RL (1994) Ca^{2+}-Calmodulin modulates ion channel activity in storage protein vacuoles of barley aleurone cells. Plant Cell 6: 277–285

Blatt MR (1992) K^+ channels of stomatal guard cells. Characteristics of the inward rectifier and its control by pH. J Gen Physiol 99: 15–644

Blatt MR, Armstrong F (1993) K^+ channels of stomatal guard cells: Abscisic-acid-evoked control of the outward rectifier mediated by cytoplasmic pH. Planta 191: 330–341

Butler A, Tsunoda S, McCobb DP, Wei A, Salkhoff L (1993) *mSlo*, a complex mouse gene encoding "maxi" calcium-activated potassium channels. Science 261: 221–224

Colombo R, Cerana R, Lado P, Peres A (1988) Voltage-dependent channels permeable to K^+ and Na^+ in the membrane of *Acer pseudoplatanus* vacuoles. J Membr Biol 103: 227–236

Colombo R, Cerana R, Lado P, Peres A (1989) Regulation by calcium of voltage-dependent tonoplast K^+ channels. Plant Physiol Biochem 27: 557–562

Colquhoun D, Sigworth FJ (1983) Fitting and statistical analysis of single-channel records. In: Sakmann B, Neher E (eds) Single channel recording. Plenum Press, London, pp 191–263

Cosgrove DJ, Hedrich R (1991) Stretch-activated chloride, potassium, and calcium channels coexisting in plasma membranes of guard cells of *Vicia faba* L. Planta 186: 143–153

Coyaud L, Kurkdjian A, Kado R, Hedrich R (1987) Ion channels and ATP-driven pumps involved in ion transport across the tonoplast of sugarbeet vacuoles. Biochim Biophys Acta 902: 263–268

DeBiasi M, Drewe JA, Kirsch GE, Brown AM (1993) Histidine substitution identifies a surface position and confers Cs^+ selectivity on a K^+ pore. Biophys J 65: 1235–1242

Evans DE, Briars SA, Williams LE (1991) Active calcium transport by plant membranes. J Exp Bot 42: 285–303

Felle H (1988a) Cytoplasmic free calcium in *Riccia fluitans* L. and *Zea mays* L.: Interaction of Ca^{2+} and pH? Planta 176: 248–255

Felle H (1988b) Short-term pH regulation in plants. Physiol Plant 74: 583–591

Felle H (1991) Aspects of Ca^{2+} homeostasis in *Riccia fluitans*: Reactions to perturbations in cytosolic-free Ca^{2+}. Plant Sci 74: 27–33

Gehring CA, Irving HR, Parish RW (1990) Effects of auxin and abscisic acid on cytosolic calcium and pH in plant cells. Proc Natl Acad Sci USA 87: 9645–9649

Gilroy S, Huges WA, Trewavas AJ (1987) Calmodulin antagonists increase free cytosolic calcium levels in plant protoplasts in vivo. FEBS Lett 212: 133–137

Goldman DE (1943) Potential, impedance and rectification in membranes. J Gen Physiol 352: 685–701

Hamill OP, Marty A, Neher E, Sakmann B, Sigworth FJ (1981) Improved patch-clamp-techniques for high-resolution current recording from cells and cell-free membrane patches. Pfluegers Arch 391: 85–100

Harper JF, Sussman MR, Schaller GE, Putnam-Evans C, Charbonneau H, Harmon AC (1991) A calcium-dependent protein kinase with a regulatory domain similar to calmodulin. Science 252: 951–954

Hedrich R, Kurkdjian A (1988) Characterization of an anion-permeable channel from sugar beet vacuoles: Effect of inhibitors. EMBO J 7: 3661–3666

Hedrich R, Marten I (1993) Malate-induced feedback regulation of plasma membrane anion channels could provide a CO_2 sensor to guard cells. EMBO J 12: 897–901

Hedrich R, Neher, E (1987) Cytoplasmic calcium regulates voltage dependent ion channels in plant vacuoles. Nature 329: 833–835

Hedrich R, Schroeder JI (1989) The physiology of ion channels and electrogenic pumps in higher plants. Annu Rev Plant Physiol 40: 539–569

Hedrich R, Schroeder JI, Fernandez JM (1986a) Patch-clamp studies on higher plant cells: A perspective. Trends Biochem Sci 12: 49–52

Hedrich R, Schroeder JI, Fernandez JM (1986b) Patch-clamp studies of ion transport in isolated plant vacuoles. FEBS Lett 3910: 228–232

Hedrich R, Barbier-Brygoo H, Felle H, Flügge UI, Lüttge U, Matthuis FJM, Marx S, Prins HBA, Raschke K, Schnabl H, Schroeder JI, Struve I, Taiz L, Ziegler P (1988) General mechanism for solute transport across the tonoplast of plant vacuoles: A patch-clamp survey of ion channels and proton pumps. Bot Acta 101: 7–13

Hedrich R, Kurkdjian A, Guern J, Flügge UI (1989) Comparative studies on the electrical properties of the H^+ translocating AT-Pase, and pyrophosphatase of the vacuolar-lysosomal compartment. EMBO J 8: 2835–2841

Hedrich R, Busch H, Raschke K (1990) Ca^{2+} and nucleotide dependent regulation of voltage dependent anion channels in the plasma membrane of guard cells. EMBO J 9: 3889–3892

Hedrich R, Marten I, Lohse G, Dietrich P, Winter H, Lohaus G, Heldt HW (1994) Malate-sensitive anion channels enable guard cells to send changes in the ambient CO_2 concentration. Plant J 6: 44–50

Hepler PK, Wayne RO (1985) Calcium and plant development. Annu Rev Plant Physiol 36: 397–439

Hille B (1992) Ionic channels of excitable membranes. Sinauer Associates Inc. Publishers, Sunderland, Massachusetts

Hodgkin AL, Katz B (1949) The effect of sodium ions on the electrical acitvity of the giant axon of the squid. J Physiol 108: 37–77

Humble GD, Raschke K (1971) Stomatal opening quantitatively related to potassium transport. Plant Physiol 48: 447–453

Ilan N, Schwartz A, Moran N (1994) External pH effects on the depolarization-activated K channels in guard cell protoplasts of *Vicia faba*. J Gen Physiol 103: 807–831

Irving HR, Gehring CA, Parish RW (1992) Changes in cytosolic pH and calcium of guard cells precede stomatal movements. Proc Natl Acad Sci USA 89: 1790–1794

Johannes E, Brosnan JM, Sanders D (1992) Parallel pathways for intracellular Ca^{2+} release from the vacuole of higher plants. Plant J 2: 97–102

Keller BU, Hedrich R, Raschke K (1989) Voltage-dependent anion channels in the plasma membrane of guard cells. Nature 341: 450–453

Lemtiri-Chlieh F, MacRobbie EAC (1994) Role of calcium in the modulation of *Vicia* guard cell potassium channels by ABA: A patch-clamp study. J Membr Biol 137: 99–107

Lewis CA (1979) Ion-concentration dependence of the reversal potential and the single channel conductance of ion channels at the frog neuromuscular junction. J Physiol 286:17–445

Llinás R, Sugimori M, Silver RB (1991) Imaging preterminal calcium concentration microdomains in the squid giant synapse. Biol Bull 181: 316–317

Maathuis FJM, Prins HBA (1991a) Patch clamp studies on root cell vacuoles of a salt-tolerant and a salt-sensitive *Plantago* species. Plant Physiol 92: 23–28

Maathuis FJM, Prins HBA (1991b) Inhibition of inward rectifying tonoplast channels by a vacuolar factor: Physiological and kinetic implications. J Membr Biol 122: 251–258

Macklon AES (1984) Calcium fluxes at plasmalemma and tonoplast. Plant Cell Environ. 7: 407–413

MacRobbie EAC (1988) Control of ion fluxes in stomatal guard cells. Bot Acta 101: 140–148

MacRobbie EAC (1990) Calcium-dependent and calcium-independent events in the initiation of stomatal closure by abscisic acid. Proc Soc Lond B 241: 214–219

Matile P (1978) Biochemistry and function of vacuoles. Annu Rev Plant Physiol 29: 193–213

Miller AJ, Sanders D (1987) Depletion of cytosolic free calcium induced by photosynthesis. Nature 326: 397–400

Neher E (1992) Corrections for liquid junction potentials in patch-clamp experiments. Methods Enzymol 207: 123–131

Pantoja O, Dainty J, Blumwald E (1989) Ion channels in vacuoles from halophytes and glycophytes. FEBS Lett 255: 92–96

Pantoja O, Gelli A, Blumwald E (1992a) Voltage-dependent calcium channels in plant vacuoles. Science 255: 1567–1570

Pantoja O, Dainty J, Blumwald E (1992b) Cytoplasmic chloride regulates cation channels in the vacuolar membrane of plant cells. J Membr Biol 125: 219–229

Penny MG, Bowling DJF (1974) A study of potassium gradients in the epidermis of intact leaves of *Commelina communis* L. in relation to stomatal opening. Planta 119: 17–25

Perry CA, Leigh RA, Tomos AD, Wyse RE, Hall JL (1987) The regulation of turgor pressure during sucrose mobilisation and salt accumulation by excised storage-root tissue of red beet. Planta 170: 353–361

Raschke K (1979) Movements of stomata. In: Haupt W, Feinleib ME (eds) Encyclopedia of plant physiology. Vol. 7: Physiology of movements. Springer Verlag, Berlin, pp 383–441

Raschke K, Hedrich R (1989) Patch clamp measurements on isolated guard cell protoplasts and vacuoles. Methods Enzymol 174: 312–329

Roberts WM, Jacobs RA, Hudspeth AJ (1990) Colocalization of ion channels involved in frequency selectivity and synaptic transmission at presynaptic active zones in hair cells. J Neurosci 10: 3664–3684

Robinson RA, Stokes RH (1959) Electrolyte solutions. Butterworths Scientific Publications, London

Sanders D, Johannes E, Hedrich R (1990) Opening plant calcium channels. Nature 344: 593–594

Schroeder JI, Hagiwara S (1989) Cytosolic calcium regulates ion channels in the plasma membrane of *Vicia faba* guard cells. Nature 338: 427–430

Schroeder JI, Hedrich R (1989) Involvement of ion channels and active transport in osmoregulation and signaling of higher plant cells. Trends Biol Sci 14: 187–192

Schroeder JI, Raschke K, Neher E (1987) Voltage dependence of K^+ channels in guard cell protoplasts. Proc Natl Acad Sci USA 84: 4108–4112

Schulz-Lessdorf B, Dietrich P, Marten I, Lohse G, Busch H, Hedrich R (1994) Coordination of plasma membrane and vacuolar membrane ion channels during stomatal movement. In: Blatt MR, Leigh RA, Sanders D (eds) Membrane transport in plants and fungi: molecular mechanisms and control (Symposia of the Society of Experimental Biology, Number XLVIII) The Company of Biologists Ltd, Cambridge, pp 99–112

Schulz-Lessdorf B, Hedrich R (1992) pH and Ca^{2+} modulate the activity of ion channels in the vacuolar membrane of guard cells–possible interaction with calmodulin. Poster Abstract [377], Botanikertagung Berlin

Siebke K, Yin ZH, Raghavendra AS, Heber U (1992) Vacuolar pH oscillations in mesophyll cells accompany oscillations of photosynthesis in leaves: Interdependence of cellular compartments, and regulation of electron flow in photosynthesis. Planta 186: 526–531

Sigworth F (1983) An example of analysis. In: Sakmann B, Neher E (eds) Single channel recording. Plenum Press, London, pp 301–321

Speer M, Kaiser WM (1991) Ion relations of symplastic and apoplastic space in leaves from *Spinacia oleracea* L. and *Pisum sativum* L. under salinity. Plant Physiol 97: 990–997

Sze H (1985) H^+-translocating ATPases: Advances using membrane vesicles. Annu Rev Plant Physiol 36: 175–208

Tarczynski MC, Outlaw WH Jr (1990) Kinetic datum collection in real time from single cell activities. Arch. Biochim Biophys 280: 71

Thuleau P, Ward JM, Ranjeva R, Schroeder JI (1994) Voltage-dependent calcium-permeable channels in the plasma membrane of a higher plant cell. EMBO J 13: 2970–2975

Wallace RW, Tallant EA, Cheung WY (1983) Assay of calmodulin by Ca^{2+}-dependent phosphodiesterase. Methods Enzymol 102: 39–46

Ward JM, Schroeder JI (1994) Calcium-activated K^+ channels and calcium-induced calcium release by slow vacuolar ion channels in guard cell vacuoles implicated in the control of stomatal closure. Plant Cell 6: 669–683

Weiser T, Bentrup FW (1990) (+)-Tubocurarine is a potent inhibitor of cation channels in the vacuolar membrane of *Chenopodium rubrum* L. FEBS Lett 277: 220–222

Weiser T, Blum W, Bentrup FW (1991) Calmodulin regulates the Ca^{2+}-dependent slow-vacuolar ion channel in the tonoplast of *Chenopodium rubrum* suspension cells. Planta 185: 440–442

Yin ZH, Neimanis S, Wagner U, Heber U (1990) Light-dependent pH changes in leaves of C_3 plants. I. Recording pH changes in various cellular compartments by fluorescent probes. Planta 182: 244–252